

Superior metabolic improvement of polycystic ovary syndrome traits after GLP1-based multi-agonist therapy

Received: 12 October 2023

Accepted: 25 September 2024

Published online: 01 October 2024

 Check for updates

Miguel A. Sánchez-Garrido ^{1,2,3,14,15} ✉, Víctor Serrano-López^{1,2,3,14}, Francisco Ruiz-Pino^{1,2,3}, María Jesús Vázquez^{1,2,3}, Andrea Rodríguez-Martín^{1,2}, Encarnación Torres^{1,2}, Inmaculada Velasco^{1,2}, Ana Belén Rodríguez^{2,4}, Eduardo Chicano-Gálvez¹, Marina Mora-Ortiz ^{1,3,5}, Claes Ohlsson ⁶, Matti Poutanen^{6,7}, Leonor Pinilla^{1,2,3,4}, Francisco Gaytán^{1,2,3,4}, Jonathan D. Douros⁸, Bin Yang⁸, Timo D. Müller^{9,10,11}, Richard D. DiMarchi ¹², Matthias H. Tschöp ^{9,10,13}, Brian Finan⁸ & Manuel Tena-Sempere ^{1,2,3,4,15} ✉

Polycystic ovary syndrome (PCOS) is a heterogeneous condition, defined by oligo-/anovulation, hyper-androgenism and/or polycystic ovaries. Metabolic complications are common in patients suffering PCOS, including obesity, insulin resistance and type-2 diabetes, which severely compromise the clinical course of affected women. Yet, therapeutic options remain mostly symptomatic and of limited efficacy for the metabolic and reproductive alterations of PCOS. We report here the hormonal, metabolic and gonadal responses to the glucagon-like peptide-1 (GLP1)-based multi-agonists, GLP1/Estrogen (GLP1/E), GLP1/gastric inhibitory peptide (GLP1/GIP) and GLP1/GIP/Glucagon, in two mouse PCOS models, with variable penetrance of metabolic and reproductive traits, and their comparison with metformin. Our data illustrate the superior efficacy of GLP1/E vs. other multi-agonists and metformin in the management of metabolic complications of PCOS; GLP1/E ameliorates also ovarian cyclicity in an ovulatory model of PCOS, without direct estrogenic uterotrophic effects. In keeping with GLP1-mediated brain targeting, quantitative proteomics reveals changes in common and distinct hypothalamic pathways in response to GLP1/E between the two PCOS models, as basis for differential efficiency. Altogether, our data set the basis for the use of GLP1-based multi-agonists, and particularly GLP1/E, in the personalized management of PCOS.

Polycystic ovary syndrome (PCOS) is the most prevalent endocrine disorder in women of reproductive age. Its prevalence ranges between 5 and 21%¹, depending on the diagnostic criteria, with higher frequency in women with obesity and specific ethnic groups^{2,3}. Its classical clinical manifestations are hyperandrogenism, ovulatory dysfunction bound to menstrual irregularities, and polycystic ovarian morphology; according to the Rotterdam criteria, PCOS is diagnosed when two of

these three clinical features concur. PCOS is considered the major cause of anovulatory infertility⁴, and is linked to other manifestations caused by androgen excess, such as hirsutism and acne. In addition, PCOS is commonly associated with metabolic disorders, such as obesity, insulin resistance, type-2 diabetes (T2D), dyslipidemia, and cardiovascular dysfunction^{5,6}. Indeed, 40–90% of women with PCOS are overweighted or obese⁷, and display insulin resistance⁸, which is also

frequently observed in lean women with PCOS, affecting roughly 60%⁸. Hence, women with PCOS are prone to T2D and cardiovascular dysfunction, increasing mortality risk.

PCOS is a heterogeneous condition in terms of pathogenesis and clinical manifestations, whose mechanisms are not fully understood. Yet, environmental, developmental, genetic, and epigenetic factors are seemingly involved⁵. The most common abnormality in PCOS is excessive ovarian androgen secretion, present in up to 80% of patients^{9,10}. Such hyperandrogenemia has a deleterious impact on ovulation and metabolic function, promoting adiposity and insulin resistance⁵. Due to this androgen-dependent alteration in insulin sensitivity, women with PCOS frequently exhibit compensatory hyperinsulinemia. Insulin has stimulatory effects on ovarian androgen production^{5,11}, and enhances the bioavailability of testosterone by decreasing the hepatic release of sex hormone-binding globulin (SHBG)¹². Such bidirectional interaction between hyperandrogenism and insulin resistance/hyperinsulinemia likely plays a key role in the pathogenesis of PCOS^{12–14}, since elevated testosterone promotes obesity and insulin resistance/hyperinsulinemia by altering body composition and insulin signaling in skeletal muscle and adipose tissue, while hyperinsulinemia contributes to increase androgen levels via ovarian-dependent mechanisms⁵.

Given the importance of hyperandrogenism-hyperinsulinemia in PCOS, most of the current therapeutic strategies aim at reducing androgen excess by improving insulin sensitivity, mainly via lifestyle changes and/or pharmacological approaches. Weight loss and improvement of insulin resistance and circulating insulin levels are considered essential for the clinical management of hyperandrogenic women with PCOS and obesity, as this may contribute to attenuating androgen excess and improve ovarian function^{5,14–16}. Thus, the first-line treatment option for PCOS is diet and exercise. However, the majority of women suffering from PCOS and obesity fail to significantly reduce their body weight with lifestyle intervention. Insulin-sensitizing drugs are the second-line treatment, with metformin being the most recommended therapeutic option, to improve peripheral insulin sensitivity in order to decrease insulin levels and, consequently, insulin-mediated stimulation of ovarian androgen secretion¹⁷. In women with PCOS and obesity, metformin has been shown to improve insulin sensitivity, reduce insulin and androgen levels, and ameliorate menstrual cyclicity and ovulation rates^{18–20}. Yet, controversial outcomes on the efficacy of metformin have also been reported^{21–24}, that might be attributed to heterogeneity of responses in some patient subgroups. Metformin has also been associated with undesired side-effects, as gastrointestinal distress, and has modest effects on body weight in women with PCOS and obesity²⁵. Further, ~5% of patients are intolerant to metformin^{18,20}. Therefore, the development of novel, safer, and more effective therapies for the clinical management of women with PCOS and their metabolic complications remains an unmet medical need.

Glucagon-like peptide-1 receptor agonists (GLP1-RA) are emerging as novel anti-diabetic and weight-loss medications for the treatment of T2D and obesity²⁶. GLP1 is a gut-derived polypeptide released from the intestinal L cells, capable of stimulating glucose-dependent insulin secretion and inhibiting food intake by acting on the pancreas and brain, respectively. In addition, GLP1 is also expressed in pancreatic alpha cells, where it exerts local insulinotropic actions²⁷. Recent, as yet fragmentary evidence suggests that intervention with GLP1-RA, e.g., liraglutide, may reduce body weight and improve hyperandrogenism and menstrual irregularities in women with obesity and PCOS^{28–32}; effects probably related to its anti-diabetic and weight-lowering properties. Of note, over the last years, an array of unimolecular GLP1-based poly-agonists, with different mechanisms of action, have been developed and experimentally validated for the treatment of metabolic syndrome, holding superior efficacy relative to conventional GLP1-RA^{33–35}. This innovative strategy of integrating the complementary actions of multiple endogenous metabolically related

hormones into a single molecule is considered one of the most promising approaches for the treatment of obesity and its comorbidities. In this context, it has been demonstrated that treatments with either a GLP1/Estrogen (GLP1/E) conjugate, a unimolecular GLP1/GIP (gastric inhibitory peptide) dual agonist, or a GLP1/GIP/Glucagon triagonist, markedly reduced body weight and improved diabetic complications, including hyperinsulinemia, in preclinical models of obesity in males^{33–35}. Yet, while their ability to reduce body weight and insulin levels was greater than GLP1 monotherapy in male models^{33–35}, the potential of these GLP1-based multi-agonists for the treatment of the metabolic, hormonal, and gonadal complications associated with PCOS has not been explored to date. Here, we document the efficacy of such unimolecular GLP1 multi-agonists, and particularly the superiority of the GLP1/E conjugate, in managing the metabolic complications of PCOS in two mouse models of the disease, with evidence also for improvement of reproductive traits in an ovulatory model of PCOS.

Results

High doses of GLP1-based multi-agonists improve metabolic function in murine models of PCOS

We explored metabolic, hormonal, and gonadal responses to different GLP1-based multi-agonists in two experimental (mouse) models of PCOS, namely PWA (postweaning androgenization) and PNA (prenatal androgenization); see Suppl. Fig. S1. Given the lack of individual preclinical models of PCOS that recapitulate all the metabolic, endocrine, and gonadal traits of the clinical syndrome, pharmacological testing was conducted in parallel in these two PCOS models, which are among the most reliable to mimic the metabolic and gonadal phenotype of women with PCOS^{36,37}, capturing also the heterogeneity of this condition³⁸. In initial validation analyses, we documented that consumption of a high-fat diet (HFD) overtly exacerbated the metabolic profile of PWA animals (Suppl. Fig. S2A, C), while in PNA mice, the impact of HFD was of similar magnitude in control and prenatally-androgenized animals (Suppl. Fig. S2B). Of note, since we aimed to test the effects of compounds against the most unfavorable metabolic conditions, we assessed the potential therapeutic utility of GLP1 multi-agonists in androgenized animals fed on HFD (Suppl. Fig. S1), which phenocopy a predominant subset of women suffering PCOS, who display overweight or obesity and may be exposed to unhealthy Western diets^{39,40}. To conduct this first pharmacological experiment, effective, high doses of the compounds, validated in preclinical models with metabolic alterations^{33–35,41,42}, were selected. Due to differences in their pharmacokinetic profiles, in this exploratory experiment, we applied a higher dose of the GLP1/E conjugate (100 nmol/kg), relative to those of the dual (GLP1/GIP) or triple (GLP1/GIP/Glucagon) agonists (10 nmol/kg).

In the PWA model, with overt metabolic and gonadal perturbations, chronic intervention with GLP1/E or the triagonist markedly reduced body weight, food intake, and circulating leptin levels (Fig. 1A–C and Suppl. Fig. S3A). This was accompanied by a considerable reduction of body fat mass and, particularly in the case of triagonist-treated mice, a substantial lowering of lean mass (Fig. 1, D). In contrast, GLP1/GIP therapy was unable to consistently reduce body weight, food intake, or fat mass in PWA mice over the study period (Fig. 1A–D). Chronic administration of GLP1/E significantly improved also glucose handling, as compared with the vehicle-treated PWA group, whereas no glucoregulatory actions were detected in mice treated with the dual or triple agonist (Fig. 1E-upper panel). Yet, animals administered with GLP1/GIP or GLP1/E displayed reduced basal glucose levels at the end of treatment (Fig. 1F). In addition, GLP1/E and GLP1/GIP/Glucagon significantly improved insulin sensitivity, as denoted by ITT and HOMA-IR index, and decreased insulin levels; effects that were not observed in GLP1/GIP-treated animals (Fig. 1E-lower panel, G, H). In PWA mice, metformin therapy caused very modest metabolic effects (Fig. 1A–G), denoted only by a moderate reduction in HOMA-IR (Fig. 1H), despite the

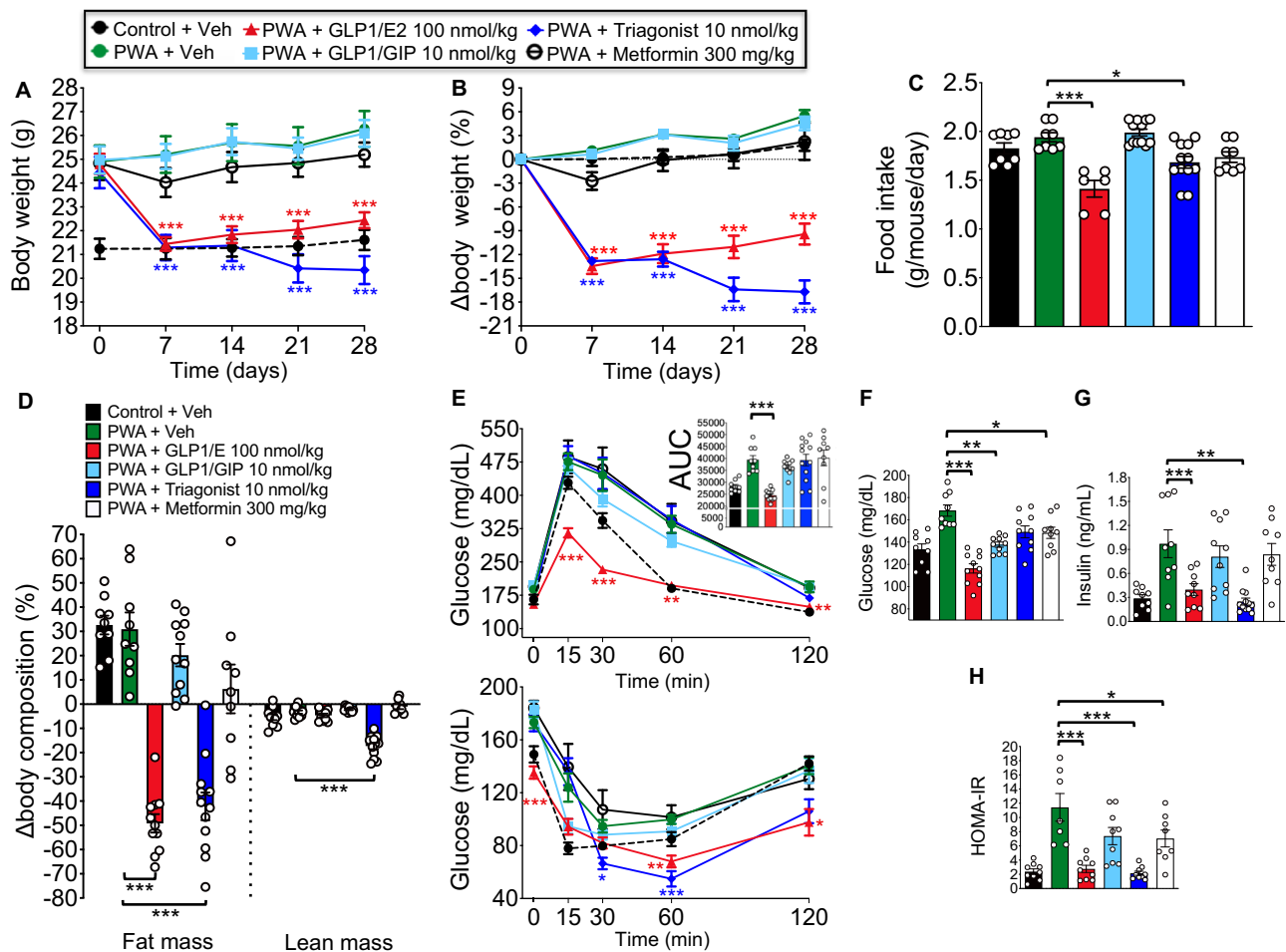


Fig. 1 | Metabolic effects of high doses of different GLP1-based multi-agonists in PWA mice. A–H Effects on body weight (A), body weight change (B), food intake (C), body composition (fat and lean mass change) (D), glucose (upper panel) and insulin tolerance (E), fasting glucose (F), serum insulin levels (G), and HOMA-IR index (H) in PWA female mice daily administered with vehicle (saline), GLP1/E (100 nmol/kg), GLP1/GIP (10 nmol/kg), GLP1/GIP/Glucagon triagonist (10 nmol/kg) or metformin (300 mg/kg) during 28 days. In order to assess integral glucose levels in the glucose tolerance test, the area under the curve (AUC) was calculated using the trapezoidal rule. Data were presented as mean \pm SEM. Group codes: Control + Veh (C); PWA + Veh (P); PWA + GLP1/E (G/E); PWA + GLP1/GIP (G/G); PWA + Triagonist (T); PWA + Metformin (M). For each panel, sample sizes (n) were as

follows: **A:** C = 10; P = 10; G/E = 11; G/G = 11; T = 11; M = 10; **B:** C = 10; P = 10; G/E = 11; G/G = 11; T = 11; M = 9; **C:** C = 8; P = 8; G/E = 6; G/G = 12; T = 12; M = 9; **D:** C = 9; P = 9; G/E = 11; G/G = 11; T = 12; M = 9; **E:** (ITT) C = 10; P = 9; G/E = 11; G/G = 11; T = 12; M = 9; **F:** C = 9; P = 9; G/E = 11; G/G = 10; T = 10; M = 9; **G:** C = 9; P = 9; G/E = 9; G/G = 10; T = 12; M = 9; **H:** C = 9; P = 7; G/E = 9; G/G = 9; T = 9; M = 8. Statistically significant differences were assessed by one-way ANOVA followed by Tukey's multiple comparison tests to analyze the effects of compound intervention vs. vehicle administration in PWA mice. For reference purposes, control non-androgenized mice are included (black bars and dashed lines). Asterisks indicate statistical significance * P < 0.05, ** P < 0.01, *** P < 0.001. Source data are provided as a Source Excel Data file (see Data availability).

dose employed was much higher (300 mg/kg) than the doses of multi-agonists. Moreover, none of the treatments altered circulating adiponectin levels, and only mice treated with triagonist showed a significant elevation in serum levels of FGF21 (Suppl. Fig. S3B, C). Regarding gonadal effects, treatment with GLP1/E, GLP1/GIP, and metformin did not alter ovarian or uterus weights, nor did they change circulating LH levels in this hyperandrogenic model of PCOS (Suppl. Fig. S3D–F). However, the triagonist caused a substantial reduction in ovarian weight and a significant drop in serum LH levels (Suppl. Fig. S3D, F). Moreover, no effects were observed in ovarian cyclicity and histology following pharmacological treatment in any of the experimental groups (Suppl. Fig. S3G).

In PNA mice, that display modest metabolic dysregulation and overt gonadal perturbations, all multi-agonists decreased body weight (Fig. 2A, B). Yet, while GLP1/E and GLP1/GIP reduced body weight by 10% at the end of the treatment, the triagonist caused a 22% reduction (Fig. 2B). As in PWA mice, such body weight loss was accompanied by a significant decrease in food intake and fat mass (Fig. 2C, D), while only mice treated with the triagonist displayed a significant reduction in

lean mass (Fig. 2D). In this PCOS model of gestational androgenization, treatment with GLP1/GIP improved glucose handling, fasting glucose levels and insulin sensitivity, as denoted by ITT and HOMA-IR, as well as circulating insulin concentrations (Fig. 2E–H), while triagonist therapy had no effects on glucose handling, but improved insulin sensitivity and reduced basal glucose levels (Fig. 2E, F, H). In contrast, high doses of GLP1/E had negligible effects on glucose control, insulin sensitivity, or circulating glucose and insulin levels (Fig. 2E–G), whereas metformin had no effects on any of the metabolic endpoints (Fig. 2A–H). Furthermore, treatment with GLP1/E, GLP1/GIP, or metformin did not modify ovarian and uterus weights, or serum LH levels; only a significant drop in serum LH concentration was detected in mice injected with GLP1/GIP (Suppl. Fig. S4A–C). In contrast, the triagonist induced a significant decrease in ovarian and uterus weight vs. vehicle-treated PNA mice (Suppl. Fig. S4A, B). Although metformin did not alter the abovementioned gonadal parameters, it improved ovarian cyclicity, as manifested by the presence of two consecutive generations of corpora lutea, vs. vehicle-injected PNA mice, which displayed clear signs of altered cyclicity, denoted by the presence of only one generation of

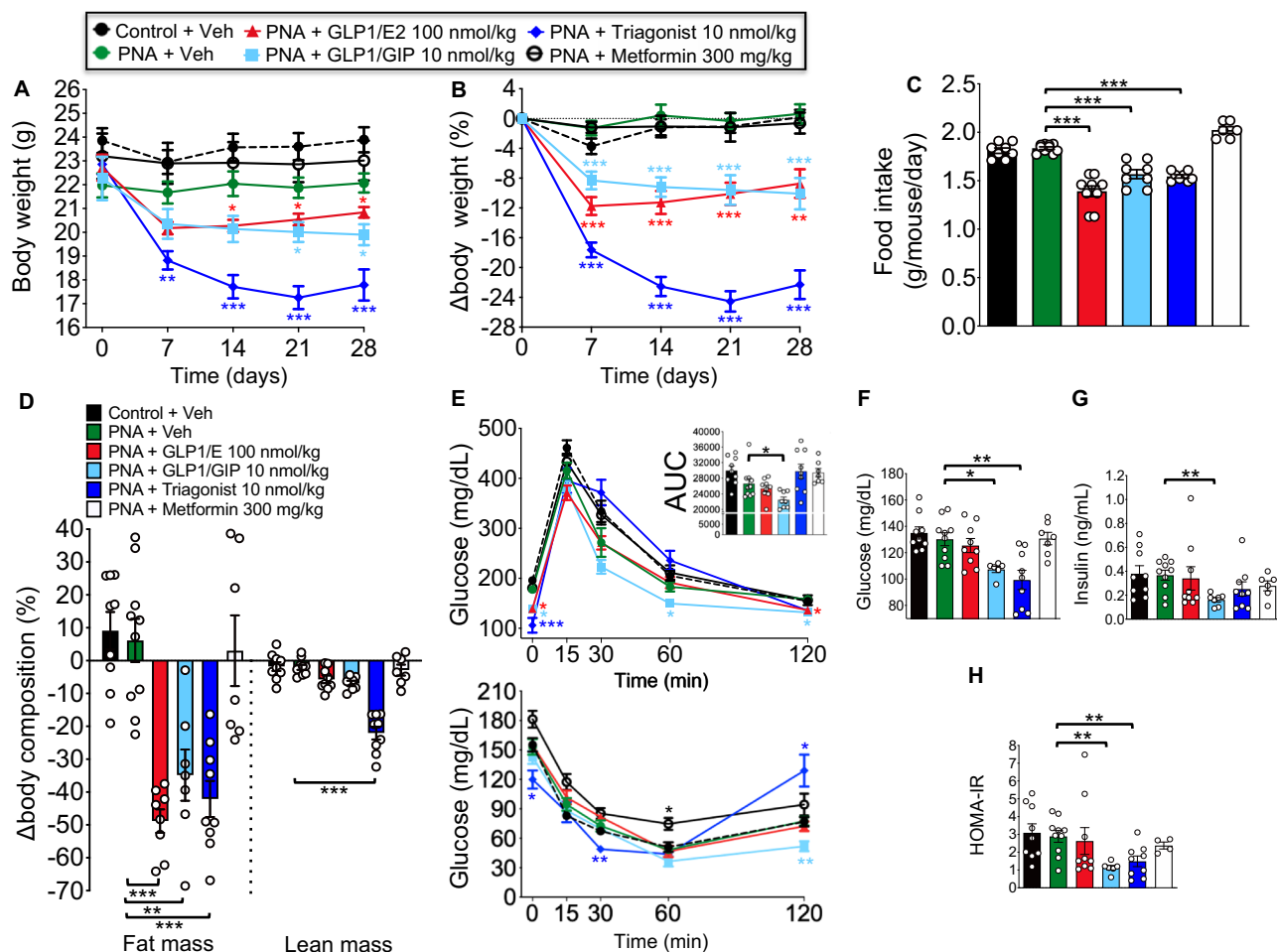


Fig. 2 | Metabolic effects of high doses of different GLP1-based multi-agonists in PNA mice. **A–H** Effects on body weight (**A**), body weight change (**B**), food intake (**C**), body composition (fat and lean mass change) (**D**), glucose (upper panel) and insulin tolerance (**E**), fasting glucose (**F**), serum insulin levels (**G**), and HOMA-IR index (**H**) in PNA female mice daily administered with vehicle (saline), GLP1/E (100 nmol/kg), GLP1/GIP (10 nmol/kg), GLP1/GIP/Glucagon triagonist (10 nmol/kg), or metformin (300 mg/kg) during 28 days. In order to assess integral glucose levels in the glucose tolerance test, the area under the curve (AUC) was calculated using the trapezoidal rule. Data were presented as mean \pm SEM. Group codes: Control + Veh (C); PNA + Veh (P); PNA + GLP1/E (G/E); PNA + GLP1/GIP (G/G); PNA + Triagonist (T); PNA + Metformin (M). For each panel, sample sizes (n) were as follows: **A:** C = 9;

P = 10; G/E = 9; G/G = 8; T = 9; M = 7; **B:** C = 9; P = 10; G/E = 9; G/G = 8; T = 9; M = 7; C = 8; P = 10; G/E = 9; G/G = 8; T = 8; M = 6; **D:** C = 9; P = 10; G/E = 9; G/G = 7; T = 9; M = 7; **E:** (GTT) C = 9; P = 10; G/E = 9; G/G = 8; T = 9; M = 7; (ITT) C = 9; P = 10; G/E = 9; G/G = 5; T = 6; M = 6; **F:** C = 9, P = 10; G/E = 9; G/G = 6; T = 9; M = 7; **G:** C = 9; P = 10; G/E = 9; G/G = 7; T = 9; M = 6; **H:** C = 9; P = 10; G/E = 9; G/G = 6; T = 9; M = 4. Statistically significant differences were assessed by one-way ANOVA followed by Tukey's multiple comparison tests to analyze the effects of compound intervention vs. vehicle administration in PNA mice. For reference purposes, control non-androgenized mice are included (black bars and dashed lines). Asterisks indicate statistical significance * $P < 0.05$, ** $P < 0.01$, *** $P < 0.001$. Source data are provided as a Source Excel Data file (see Data availability).

corpora lutea, frequently corresponding to persistent regressing corpora lutea, indicative of occasional ovulations. In contrast, no effects on ovarian function were observed after treatment with high doses of the different multi-agonists in this PCOS model (Suppl. Fig. S4D).

Superior metabolic improvement by GLP1/E vs. dual and triple multi-agonists in PCOS models

We next scaled down the doses of the poly-agonists in both PCOS models: 50 nmol/kg of GLP1/E and 3 nmol/kg of the dual and triple agonists, as selected according to previous references^{33–35}. In PWA mice, treatment with GLP1/E caused a significant decrease in body weight (10%) and fat mass (50%), as well as a reduction in food intake and substantial improvement in glucose metabolism and insulin sensitivity, denoted by ITT and HOMA-IR, as well as serum glucose, insulin (Fig. 3A–H) and leptin levels (Suppl. Fig. S5A). In contrast, the low dose of GLP1/GIP failed to persistently improve body weight, body composition, or food intake, but significantly ameliorated glucose handling and insulin sensitivity, and reduced basal glucose levels vs. the vehicle-treated PWA group (Fig. 3A–H). Triagonist-treated mice showed a slight

reduction of body weight along treatment (2%) and improved glucose tolerance, although no changes were detected in the other metabolic parameters analyzed (Fig. 3A–H and Suppl. Fig. S5A–C). As in previous experiments, intervention with an effective dose of metformin had minimal effects on the metabolic profile (Fig. 3A–G), except for marginal improvement of insulin resistance, denoted by a modest reduction of HOMA-IR (Fig. 3H). No changes in lean mass were observed after chronic treatment with the lower doses of any of the poly-agonists (Fig. 3D). No significant alterations were detected either in circulating FGF21 or adiponectin levels (Suppl. Fig. S5B, C). Finally, none of the multi-agonists at lower doses, nor metformin, had a beneficial effect on ovarian cyclicity or any other gonadal parameter, such as ovarian and uterus weights and circulating LH levels (Suppl. Fig. S5D–F).

In PNA mice, treatment with the lower dose of GLP1/E had also superior metabolic efficacy vs. GLP1/GIP and the triple-agonist, promoting a sustained and significant decrease in body weight (8%), a marked reduction in fat tissue ($\approx 40\%$) and food intake, as well as an improvement in glucose metabolism (Fig. 4A–H). In contrast, the metabolic profile PNA mice was unaffected after intervention with

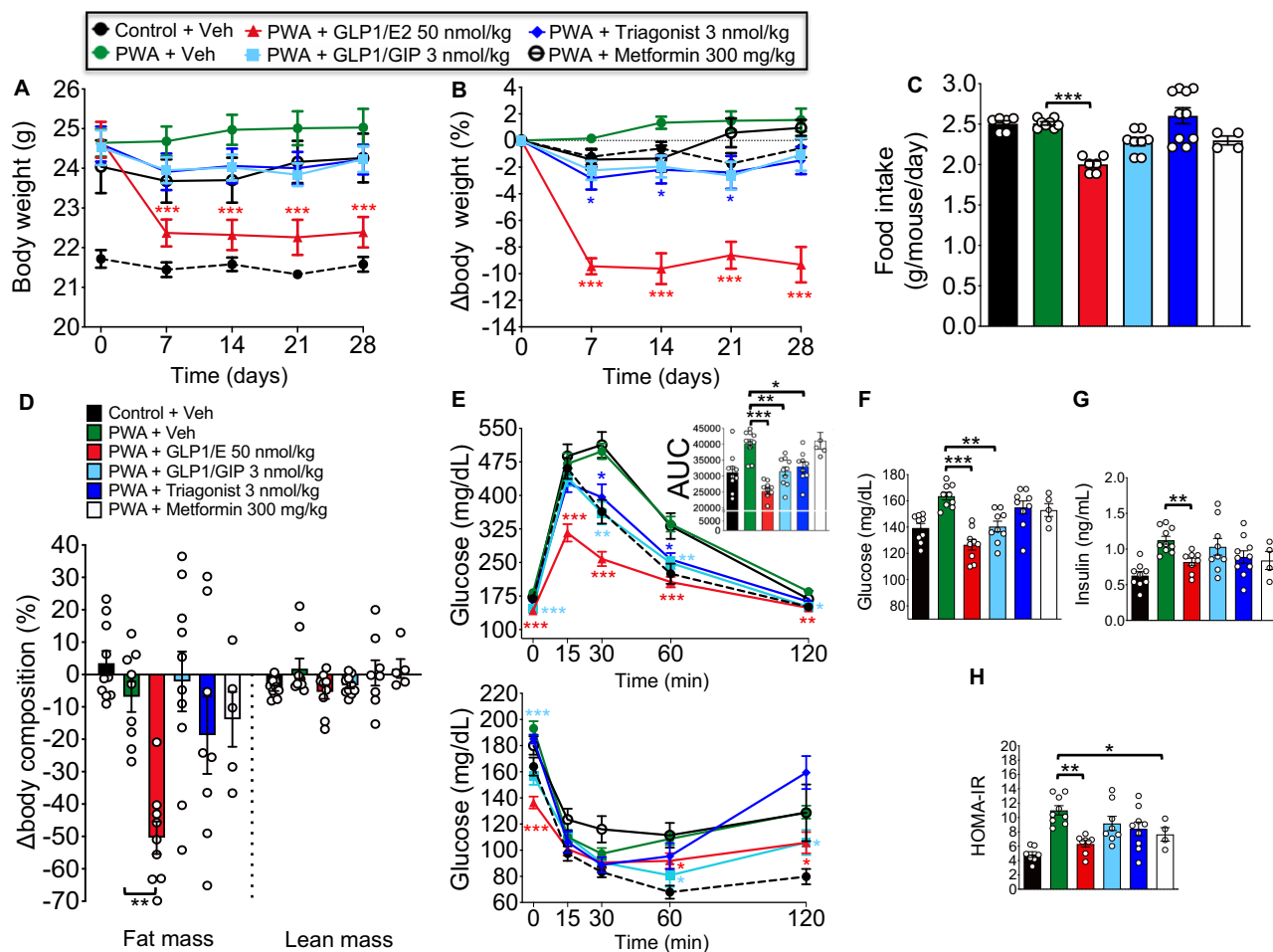


Fig. 3 | Metabolic effects of lower doses of different GLPI-based multi-agonists in PWA mice.

A–H Effects on body weight (**A**), body weight change (**B**), food intake (**C**), body composition (fat and lean mass change) (**D**), glucose (upper panel) and insulin tolerance (**E**), fasting glucose (**F**), serum insulin levels (**G**), and HOMA-IR index (**H**) in PWA female mice daily administered with vehicle (saline), GLP1/E (50 nmol/kg), GLP1/GIP (3 nmol/kg), GLP1/GIP/Glucagon triagonist (3 nmol/kg) or metformin (300 mg/kg) during 28 days. In order to assess integral glucose levels in the glucose tolerance test, the area under the curve (AUC) was calculated using the trapezoidal rule. Data were presented as mean \pm SEM. Group codes: Control + Veh (C); PWA + Veh (P); PWA + GLP1/E (G/E); PWA + GLP1/GIP (G/G); PWA + Triagonist (T); PWA + Metformin (M). For each panel, sample sizes (n) were as follows: A:

C = 11; P = 10; G/E = 10; G/G = 10; T = 10; M = 5; **B**: C = 11; P = 10; G/E = 10; G/G = 10; T = 10; M = 5; **C**: C = 6; P = 8; G/E = 6; G/G = 8; T = 10; M = 4; **D**: C = 10; P = 9; G/E = 9; G/G = 10; T = 8; M = 5; **E**: (GTT & ITT) C = 11; P = 10; G/E = 10; G/G = 10; T = 10; M = 5; **F**: C = 9; P = 9; G/E = 9; G/G = 9; T = 9; M = 5; **G**: C = 9; P = 10; G/E = 8; G/G = 9; T = 10; M = 4; **H**: C = 7; P = 9; G/E = 8; G/G = 8; T = 9; M = 4. Statistically significant differences were assessed by one-way ANOVA followed by Tukey's multiple comparison tests to analyze the effects of compound intervention vs. vehicle administration in PWA mice. For reference purposes, control non-androgenized mice are included (black bars and dashed lines). Asterisks indicate statistical significance * $P < 0.05$, ** $P < 0.01$, *** $P < 0.001$. Source data are provided as a Source Excel Data file (see Data availability).

lower doses of the dual- and triple-agonists, as well as with metformin (Fig. 4A–H), except for a significant decrease in basal glucose levels in GLP1/GIP-treated mice (Fig. 4F) and reduction in daily food intake in PNA mice treated with metformin (Fig. 4C). None of the compounds at low doses caused changes in lean mass (Fig. 4D). Concerning the gonadal profile, no changes were detected in any of the reproductive endpoints after treatment with the lower doses of the poly-agonists (Suppl. Fig. S6A–C).

GLP1/E, at very low doses, is sufficient to ameliorate PCOS-associated metabolic alterations

Since GLP1/E was superior to any other compound in terms of improvement of metabolic traits, we next assessed the metabolic efficacy of very low doses of this multi-agonist in our metabolically dysregulated PCOS model. To this end, we performed a dose-finding study in PWA mice, as model with more severe metabolic alterations, testing the doses of 5, 10, and 25 nmol/kg of GLP1/E. The three doses of GLP1/E led to a very significant reduction of body weight along the treatment period (Fig. 5A), with a 10% drop in body weight for the

highest dose, and an 8% reduction with the 10 and 5 nmol/kg doses relative to vehicle-treated PWA mice (Fig. 5B). Daily treatment with these doses of GLP1/E also reduced food intake; an effect that reached statistical significance with the 10 and 25 nmol/kg doses (Fig. 5C). In good agreement, mice treated with GLP1/E displayed significant loss of fat mass, which was greater in animals exposed to the intermediate and high doses (Fig. 5D), together with a pronounced reduction in leptin levels (Suppl. Fig. S7A). No changes in lean mass were detected after intervention with the different doses of GLP1/E (Fig. 5D). In addition, mice treated with any of the three low doses of GLP1/E displayed improved glucose handling and basal glucose levels, with higher responses in mice treated with 10 and 25 nmol/kg doses (Fig. 5E, F). GLP1/E significantly ameliorated also insulin sensitivity, as denoted by ITT and HOMA-IR, regardless of the dose, and reduced basal insulin levels (Fig. 5E, G, H); yet, the latter was significant only in mice treated with the highest dose. GLP1/E did not alter adiponectin or FGF21 levels at any dose (Suppl. Fig. S7B, C). As in previous experiments in PWA mice, no effects on the gonadal profiles were found after treatments with GLP1/E, independently of the dose (Suppl. Fig. S7D–F).

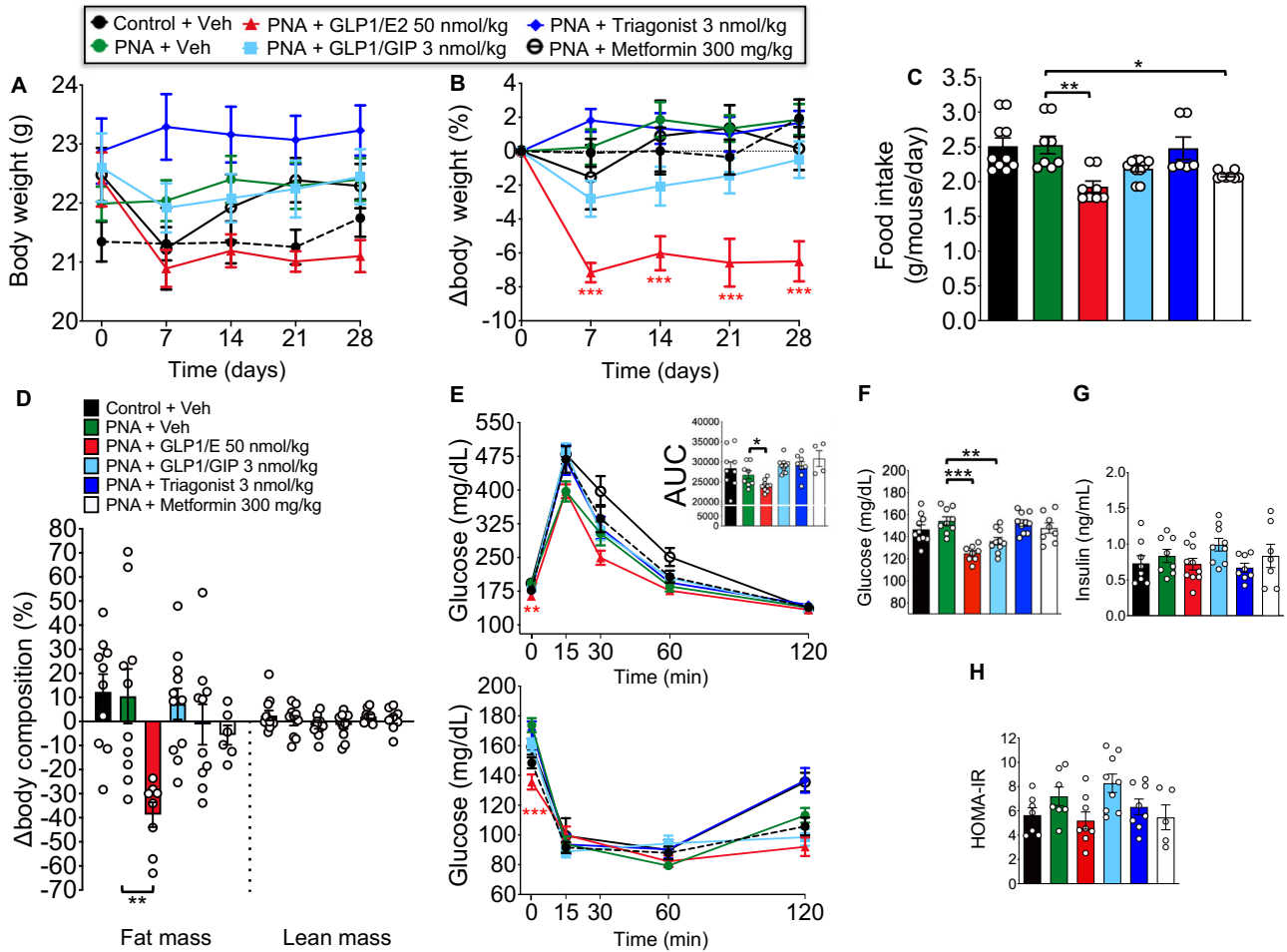


Fig. 4 | Metabolic effects of lower doses of different GLPI-based multi-agonists in PNA mice. A–H Effects on body weight (A), body weight change (B), food intake (C), body composition (fat and lean mass change) (D), glucose (upper panel) and insulin tolerance (E), fasting glucose (F), serum insulin levels (G), and HOMA-IR index (H) in PNA female mice daily administered with vehicle (saline), GLP1/E (50 nmol/kg), GLP1/GIP (3 nmol/kg), GLP1/GIP/Glucagon triagonist (3 nmol/kg) or metformin (300 mg/kg) during 28 days. In order to assess integral glucose levels in the glucose tolerance test, the area under the curve (AUC) was calculated using the trapezoidal rule. Data were presented as mean \pm SEM. Group codes: Control + Veh (C); PNA + Veh (P); PNA + GLP1/E (G/E); PNA + GLP1/GIP (G/G); PNA + Triagonist (T); PNA + Metformin (M). For each panel, sample sizes (*n*) were as follows: A: C = 11;

P = 10; G/E = 10; G/G = 11; T = 10; M = 9; B: C = 11; P = 10; G/E = 9; G/G = 11; T = 10; M = 7; C: C = 10; P = 8; G/E = 8; G/G = 10; T = 6; M = 8; D: C = 10; P = 10; G/E = 8; G/G = 11; T = 10; M = 6; E: (GTT) C = 8; P = 8; G/E = 8; G/G = 8; T = 9; M = 8; (ITT) C = 10; P = 10; G/E = 10; G/G = 11; T = 10; M = 9; F: C = 10; P = 9; G/E = 8; G/G = 10; T = 10; M = 8; G: C = 8; P = 8; G/E = 10; G/G = 9; T = 8; M = 7; H: C = 7; P = 7; G/E = 8; G/G = 9; T = 8; M = 5. Statistically significant differences were assessed by one-way ANOVA followed by Tukey's multiple comparison tests to analyze the effects of compound intervention vs. vehicle administration in PNA mice. For reference purposes, control non-androgenized mice are included (black bars and dashed lines). Asterisks indicate statistical significance **P* < 0.05, ***P* < 0.01, ****P* < 0.001. Source data are provided as a Source Excel Data file (see Data availability).

Multi-agonist therapy is not bound to gastrointestinal distress in an obese model of PCOS

To explore potential gastrointestinal distress linked to multi-agonist interventions, as a putative bias for interpretation of their effects, we conducted kaolin tests in PWA mice. Pica behavior is a validated endpoint to assess the ability of a compound to induce nausea/malaise in non-vomiting species, as mouse, based on the monitoring of non-nutritive (kaolin) food intake, as an index of gastrointestinal discomfort^{43,44}. We assessed equimolar (10 nmol/kg) and effective doses of GLP1/E, GLP1/GIP, and GLP1/GIP/Glucagon, as documented in our previous pharmacological tests; body weight, food intake, and kaolin consumption were monitored along the first 72 h of treatments in PWA mice fed on HFD. We also included a group treated with GLP1 analog (10 nmol/kg). Treatments with any of the multi-agonists significantly reduced body weight from 24- to 72-h relative to control PWA animals, while GLP1 decreased body weight only from 24- to 48-h; the magnitude of such effect was much lower than of multi-agonists (Suppl. Fig. S8A). In good agreement, intervention with the multi-agonists significantly

reduced food intake from 2- to 72-h, while the anorectic effects of GLP1 manifested only from 2- to 24-h (Suppl. Fig. S8B). Notably, treatments with the multi-agonists or GLP1 did not cause signs of nausea/malaise at any time-point tested (2–72 h), since pica behavior (i.e., kaolin intake) was similar, or even lower, in mice treated with GLP1/E, GLP1/GIP, GLP1/GIP/Glucagon, or GLP1 vs. the control PWA group (Suppl. Fig. S8C).

The body weight-lowering effects of multi-agonists are primarily due to their anorectic actions

As multi-agonist therapies elicited a marked reduction in body weight during the first week of treatment, we assessed the putative mechanisms associated with such weight loss. To this end, we applied indirect calorimetry and infrared thermography systems in PWA mice, treated with equimolar doses (10 nmol/kg) of GLP1/E, GLP1/GIP, and GLP1/GIP/Glucagon, during the first 3 days of treatment; a period when body weight loss was particularly marked. Treatment with the multi-agonists caused a very significant reduction in body weight during the 72-h treatment period, which was more pronounced in

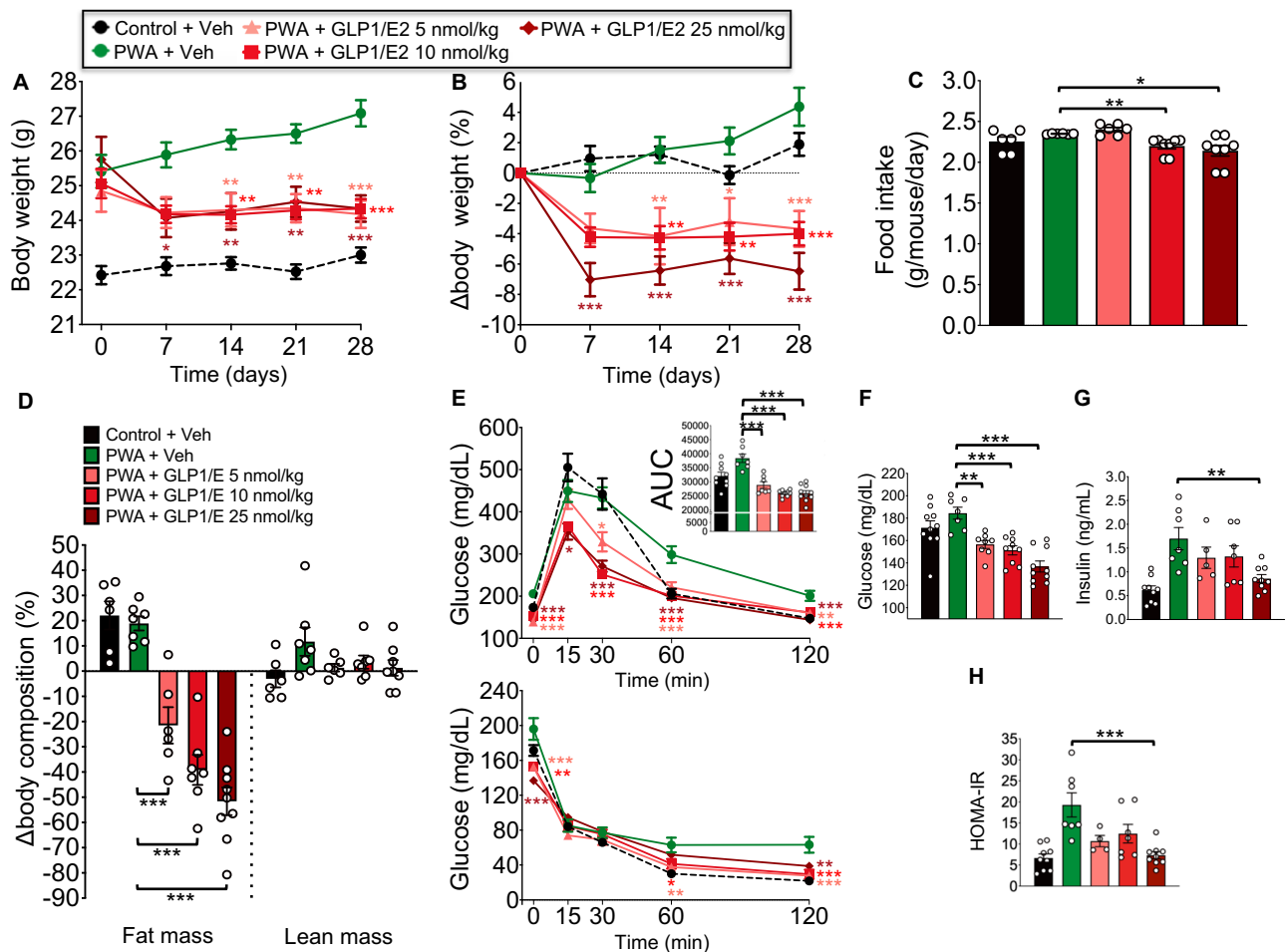


Fig. 5 | Metabolic effects of very low doses of GLP1/E in PWA mice. A–H Effects on body weight (A), body weight change (B), food intake (C), body composition (fat and lean mass change) (D), glucose (upper panel) and insulin tolerance (E), fasting glucose (F), serum insulin levels (G), and HOMA-IR index (H) in PWA female mice daily administered with vehicle (saline) or GLP1/E (5, 10, and 25 nmol/kg) during 28 days. In order to assess integral glucose levels in the glucose tolerance test, the area under the curve (AUC) was calculated using the trapezoidal rule. Data were presented as mean \pm SEM. Group codes: Control + Veh (C); PWA + Veh (P); PWA + GLP1/E 5 nmol/kg (G/E5); PWA + GLP1/E10 nmol/kg (G/E10); PWA + GLP1/E25 nmol/kg (G/E25). For each panel, sample sizes (n) were as follows: A: C = 10; P = 7; G/E5 = 8; G/E10 = 8; G/E25 = 10; B: C = 9; P = 7; G/E5 = 8; G/E10 = 8; G/E25 = 9; C: C = 6; P = 6; G/

E5 = 6; G/E10 = 8; G/E25 = 8; D: C = 6; P = 7; G/E5 = 6; G/E10 = 7; G/E25 = 9; E: (GTT) C = 9; P = 8; G/E5 = 8; G/E10 = 9; G/E25 = 10; (ITT) C = 10; P = 8; G/E5 = 9; G/E10 = 8; G/E25 = 10; F: C = 10; P = 7; G/E5 = 8; G/E10 = 9; G/E25 = 10; G: C = 9; P = 7; G/E5 = 5; G/E10 = 7; G/E25 = 9; H: C = 9; P = 7; G/E5 = 4; G/E10 = 7; G/E25 = 9. Statistically significant differences were assessed by one-way ANOVA followed by Tukey's multiple comparison tests to analyze the effects of compound intervention vs. vehicle administration in PWA mice. For reference purposes, control non-androgenized mice are included (black bars and dashed lines). Asterisks indicate statistical significance * P < 0.05, ** P < 0.01, *** P < 0.001. Source data are provided as a Source Excel Data file (see Data availability).

mice treated with GLP1/GIP/Glucagon (Fig. 6A). The decrease in body weight was associated with a significant reduction in food intake from 24- to 72-h in all the treatment groups, although the anorectic effects of the triagonist were greater (Fig. 6B). Conversely, intervention with the multi-agonists did not alter mean energy expenditure or locomotor activity in this PCOS model (Fig. 6C, D), suggesting that, at least in the initial phase of treatment, these compounds drive their weight-lowering effects mostly by reducing food consumption, without inducing thermogenic responses. Multi-agonist therapy altered respiratory quotient, promoting greater fat oxidation (Fig. 6E), while infrared thermography revealed that treatment with none of the multi-agonists enhanced interscapular temperature (Fig. 6F, G).

Superior metabolic efficacy of GLP1/E vs. GLP1 or E monotherapies in an obese model of PCOS

Since the 10 nmol/kg dose of GLP1/E was at least as effective as higher doses in improving the metabolic profile of PCOS mice, we compared its beneficial effects in terms of body weight, fat mass, glucose

tolerance, insulin sensitivity, and other traits vs. each single constituent of the conjugate, namely GLP1 and estrogen (E). PWA mice were administered with equimolar doses of GLP1, E, or GLP1/E (10 nmol/kg), and results were compared with those of vehicle- or metformin-treated (300 mg/kg) PWA mice. GLP1 alone significantly reduced body weight and fat mass, and improved glucose handling, as well as serum glucose and insulin concentrations, and insulin sensitivity in this PCOS model (Fig. 7A–H), together with a decrease in circulating leptin levels (Suppl. Fig. S9A). A similar dose of E caused a slight reduction in body weight and fat mass, as well as a significant improvement in glucose tolerance and glucose levels (Fig. 7A–G), as well as a non-significant lowering of circulating leptin (Suppl. Fig. S9A). However, treatment with equimolar doses of GLP1/E markedly improved body weight, food intake, fat mass, leptin levels, glucose metabolism, insulin sensitivity, and circulating insulin levels with far superior efficacy as compared with GLP1 and E monotherapies (Fig. 7A–H and Suppl. Fig. S9A). On the other hand, metformin-treated mice displayed a slight decrease in body weight, fat mass, and circulating glucose, insulin, and leptin levels, which was associated with a

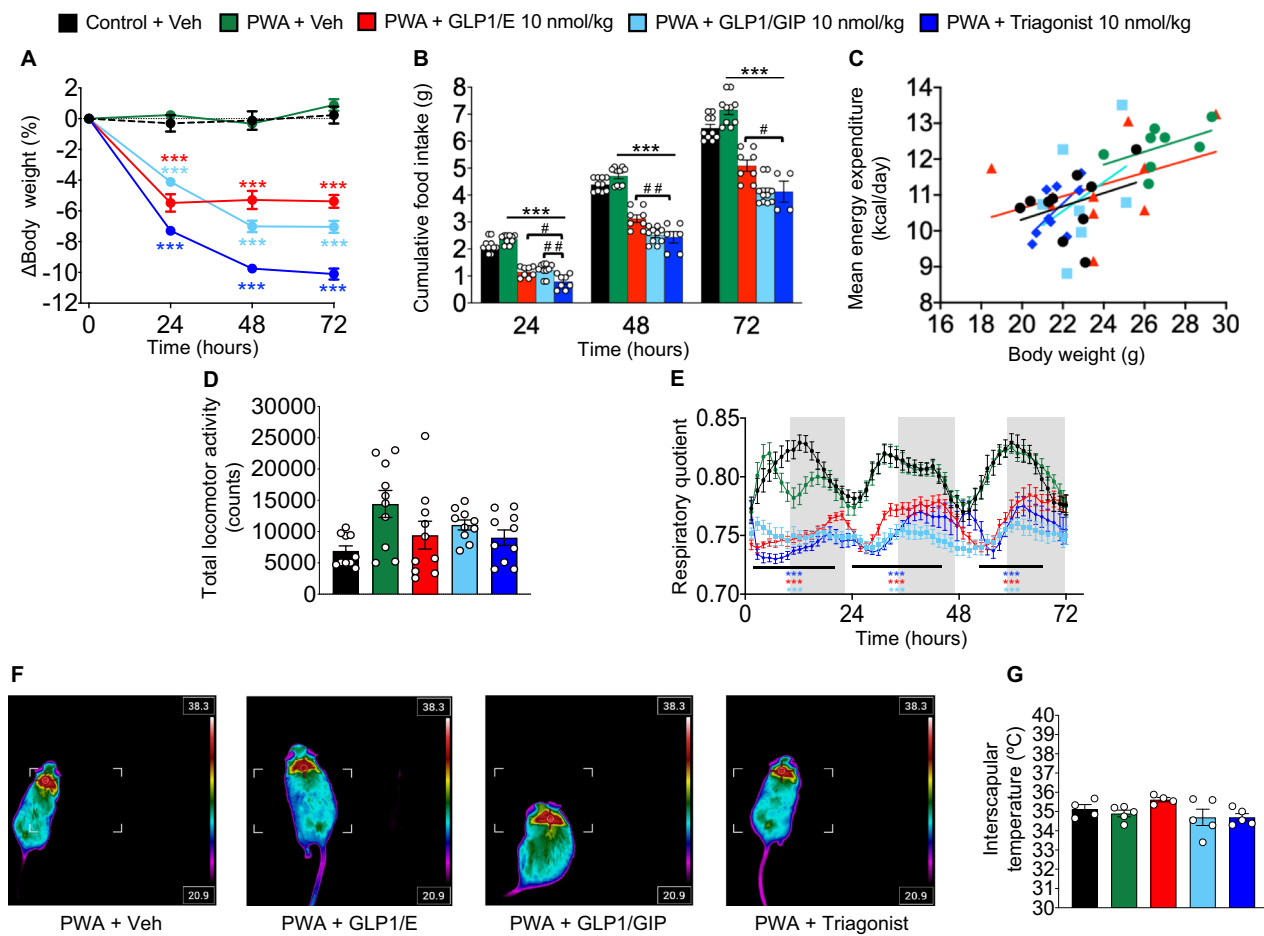


Fig. 6 | Short-term metabolic effects of GLP1-based multi-agonists in PWA mice. **A–G** Effects on body weight change (**A**), food intake (**B**), body weight-correlated average energy expenditure (**C**), total locomotor activity (**D**), and respiratory quotient (**E**) in PWA female mice daily treated with vehicle, GLP1/E (10 nmol/kg), GLP1/GIP (10 nmol/kg), triagonist (10 nmol/kg), during 3 days. In addition, representative images and mean interscapular temperature (**F**, **G**) of the different experimental groups are shown. Data were presented as mean \pm SEM. Group codes: Control + Veh (C); PWA + Veh (P); PWA + GLP1/E (G/E); PWA + GLP1/GIP (G/G); PWA + Triagonist (T). For each panel, sample sizes (n) were as follows: **A**: C = 10; P = 10; G/E = 10; G/G = 10; T = 9; **B**: C = 10; P = 10; G/E = 8; G/G = 10; T = 8; **C**: C = 10;

P = 8; G/E = 10; G/G = 7; T = 9; **D**: C = 10; P = 10; G/E = 10; G/G = 10; T = 10; **E**: C = 10; P = 10; G/E = 10; G/G = 10; T = 10; **G**: C = 4; P = 5; G/E = 4; G/G = 5; T = 5. Statistically significant differences were assessed by one-way ANOVA followed by Tukey's multiple comparison tests to analyze the effects of compound intervention vs. vehicle administration in PWA mice. For reference purposes, control non-androgenized mice are included (black bars and dashed lines). Asterisks indicate statistical significance * $P < 0.05$, ** $P < 0.01$, *** $P < 0.001$ compared to PWA + Veh. Number sign indicate statistical significance # $P < 0.05$, ## $P < 0.01$, compared to PWA + Triagonist. Source data are provided as a Source Excel Data file (see Data availability).

modest reduction of HOMA-IR index and a drop in daily food intake (Fig. 7A–H and Suppl. Fig. S9A). As in previous experiments in PWA mice, no gonadal effects were detected following treatment with the different drugs, except for a significant reduction in ovarian weight and an increase in uterus weight in E-treated mice (Suppl. Fig. S9D–G). As internal control, in PWA mice, generated by chronic exposure to exogenous DHT, circulating levels of this androgen were consistently elevated, without differences among the different experimental groups (Suppl. Table S1, upper panel). None of the compounds caused changes in testosterone levels, except for a modest but significant increase in GLP1-treated PWA mice (Fig. 7I).

GLP1/E improves metabolic and gonadal traits in a PCOS model of ovarian dysfunction

We next assessed the metabolic, gonadal, and hormonal effects of the intervention with equivalent doses (10 nmol/kg) of GLP1, E, or GLP1/E in PNA mice, which retain ovulatory capacity albeit with clear dysregulation of ovarian cyclicity. Chronic administration of GLP1 decreased body weight, fat mass, and food intake, whereas no glucoregulatory or insulin-sensitizing actions were detected (Fig. 8A–H), while treatment with a similar dose of E improved only insulin

sensitivity (Fig. 8A–H). As in the PWA model, the improvement caused by GLP1/E therapy in PNA mice in terms of body weight, fat mass, food intake, and insulin sensitivity largely exceeded that of GLP1 or E monotherapies (Fig. 8A–H). In contrast, metformin did not cause significant changes in any of the metabolic parameters under analysis (Fig. 8A–H). Unlike the PWA model, circulating DHT levels were nearly undetectable and unaltered in PNA mice, regardless of the treatment (Suppl. Table S1, lower panel). However, GLP1/E reduced testosterone levels in PNA mice, an effect mimicked by monotherapies and metformin (Fig. 8I); a similar profile was detected for serum levels of progesterone (Suppl. Table S1, lower panel).

In the PNA model, chronic exposure to metformin substantially improved ovarian cyclicity. Thus, while up to 70% of PNA mice displayed irregular cyclicity, characterized by the appearance of only one generation of (mainly persistent regressing) corpora lutea, 100% of PNA mice treated with metformin showed regular ovarian cyclicity, denoted by the presence of two generations of corpora lutea, as a sign of preserved regular ovulations (Fig. 9A–C). Treatment with a 10 nmol/kg dose of GLP1 also ameliorated estrous cyclicity, with 80% of PNA mice showing regular cycles (Fig. 9A–C), although no effects were seen in the rest of gonadal and hormonal parameters (Fig. 9D–G). Likewise,

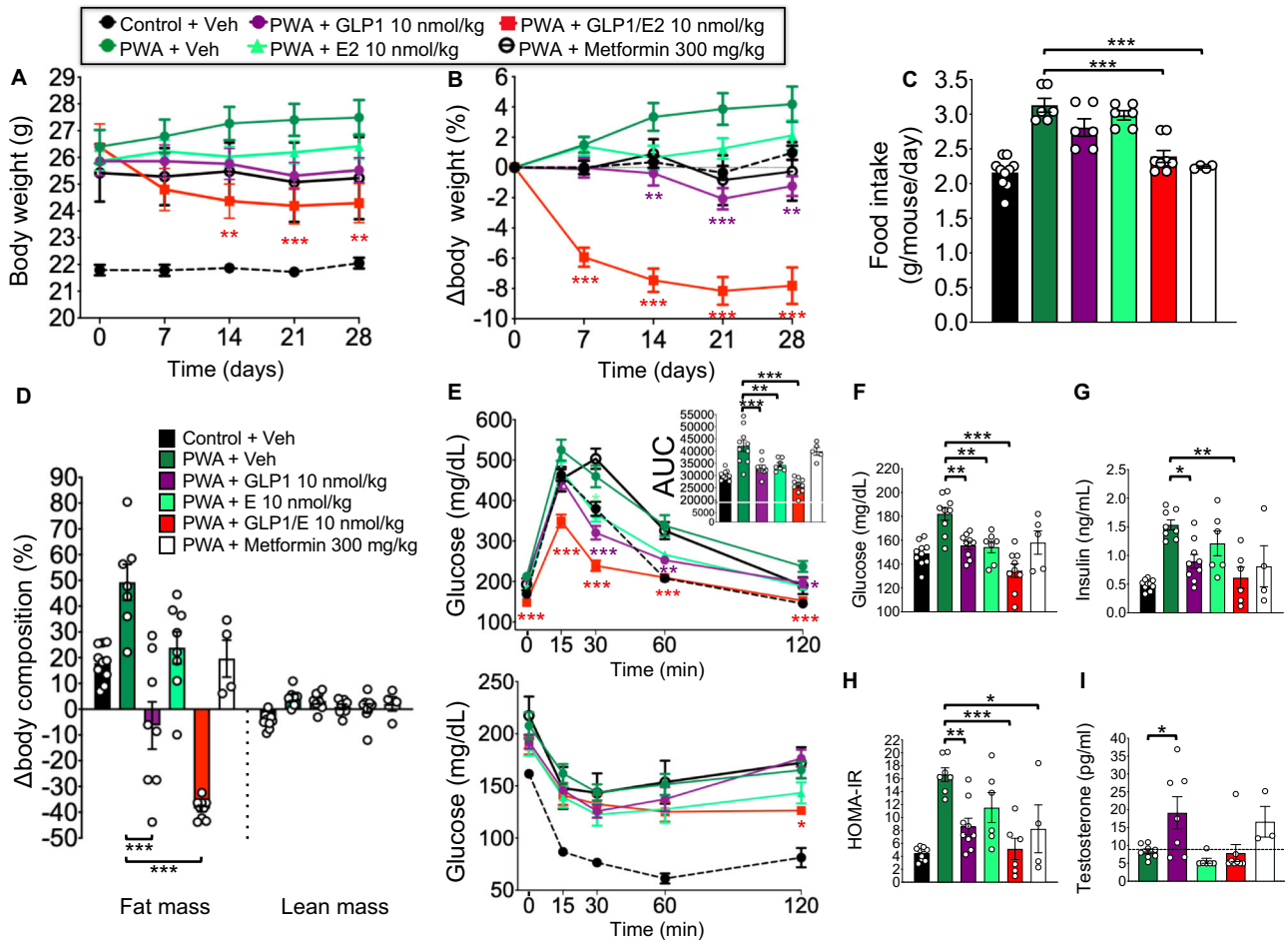


Fig. 7 | Metabolic and endocrine effects of equivalent doses of GLP1, E, or GLP1/E in PWA mice. **A–I** Effects on body weight (**A**), body weight change (**B**), food intake (**C**), body composition (fat and lean mass change) (**D**), glucose (upper panel) and insulin tolerance (**E**), fasting glucose (**F**), serum insulin levels (**G**), HOMA-IR index (**H**), and serum testosterone concentrations (**I**) in PWA female mice daily administered with vehicle (saline), GLP1 (10 nmol/kg), estrogen (E, 10 nmol/kg), GLP1/E (10 nmol/kg), or metformin (300 mg/kg) during 28 days. In order to calculate integral glucose levels in the glucose tolerance test, the area under the curve (AUC) was calculated using the trapezoidal rule. Data were presented as mean ± SEM. Group codes: Control + Veh (C); PWA + Veh (P); PWA + GLP1 (G); PWA + E (E); PWA + GLP1/E (G/E); PWA + Metformin (M). For each panel, sample sizes (*n*) were as follows: **A:** C = 10; P = 9; G = 9; E = 8; G/E = 9; M = 5; **B:** C = 10; P = 9; G = 9; E = 8; G/E = 9; M = 4; **C:** C = 10; P = 6; G = 6; E = 6; G/E = 8; M = 4; **D:** C = 10; P = 7; G = 8; E = 8; G/E = 9; M = 4; **E:** (GTT) C = 10; P = 10; G = 9; E = 7; G/E = 10; M = 5; (ITT) C = 10; P = 9; G = 8; E = 8; G/E = 9; M = 5; **F:** C = 10; P = 9; G = 9; E = 7; G/E = 9; M = 5; **G:** C = 10; P = 8; G = 9; E = 6; G/E = 6; M = 4; **H:** C = 10; P = 7; G = 9; E = 6; G/E = 6; M = 4; **I:** P = 8; G = 7; E = 6; G/E = 8; M = 3. Statistically significant differences were assessed by one-way ANOVA followed by Tukey's multiple comparison tests to analyze the effects of compound intervention vs. vehicle administration in PWA mice. For reference purposes, values from control non-androgenized mice are also included (black bars and dashed lines). Asterisks indicate statistical significance **P* < 0.05, ***P* < 0.01, ****P* < 0.001. Source data are provided as a Source Excel Data file (see Data availability).

G/E = 9; M = 4; **C:** C = 10; P = 6; G = 6; E = 6; G/E = 8; M = 4; **D:** C = 10; P = 7; G = 8; E = 8; G/E = 9; M = 4; **E:** (GTT) C = 10; P = 10; G = 9; E = 7; G/E = 10; M = 5; (ITT) C = 10; P = 9; G = 8; E = 8; G/E = 9; M = 5; **F:** C = 10; P = 9; G = 9; E = 7; G/E = 9; M = 5; **G:** C = 10; P = 8; G = 9; E = 6; G/E = 6; M = 4; **H:** C = 10; P = 7; G = 9; E = 6; G/E = 6; M = 4; **I:** P = 8; G = 7; E = 6; G/E = 8; M = 3. Statistically significant differences were assessed by one-way ANOVA followed by Tukey's multiple comparison tests to analyze the effects of compound intervention vs. vehicle administration in PWA mice. For reference purposes, values from control non-androgenized mice are also included (black bars and dashed lines). Asterisks indicate statistical significance **P* < 0.05, ***P* < 0.01, ****P* < 0.001. Source data are provided as a Source Excel Data file (see Data availability).

GLP1/E also improved estrous cyclicity and promoted the presence of two generations of corpora lutea in PNA animals, to a comparable magnitude to that observed for GLP1 monotherapy (Fig. 9A–C). In addition, GLP1/E intervention significantly increased serum LH levels and slightly reduced circulating AMH levels, without altering ovarian and uterus weights (Fig. 9D–G). Conversely, E treatment alone failed to normalize estrous cyclicity in the PNA model, as 63% of E-treated PNA mice displayed clear signs of perturbed ovarian cyclicity (Fig. 9B). E monotherapy did not alter serum LH and AMH levels, or ovarian weight, but significantly increased uterus weights (Fig. 9D–H). Importantly, this uterotrophic effect was not observed in GLP1/E-treated PNA mice (Fig. 9G, H).

Distinct alterations of hypothalamic proteomic profiles by GLP1/E in lean and obese PCOS mice

Finally, considering that the hypothalamus is likely the primary target of the GLP1/E conjugate, we assessed changes in global hypothalamic proteome in PWA and PNA mice following GLP1/E treatment, using

cutting-edge liquid chromatography–tandem mass spectrometry (LC-MS/MS). Raw data obtained from LC-MS/MS were processed, filtered, and normalized as described in the methods section. Heatmaps generated using Ward clustering and Euclidean distance measurement revealed distinct patterns of protein expression between treated and control groups in both PWA and PNA models. In PWA groups, heatmaps displayed a clear separation between PWA + Vehicle and PWA + GLP1/E, indicating substantial alterations in proteomic profiles upon treatment, with both increased and decreased proteins being observed in the treated group (Fig. 10A–left panel). Similarly, in the PNA group, a marked difference in expression patterns was observed between PNA + Vehicle and PNA + GLP1/E conditions, with a noticeable reduction in protein expression in GLP1/E-treated mice (Fig. 10A–right panel). Volcano plots further highlighted the differential protein profiles induced by GLP1/E treatment. In the PWA group, several proteins were significantly upregulated (red dots) or downregulated (blue dots) when comparing PWA + GLP1/E to PWA + Vehicle, with an FDR threshold of 0.1 (Fig. 10B–left panel). Notably, proteins such as MRPS36 and RNF181 were

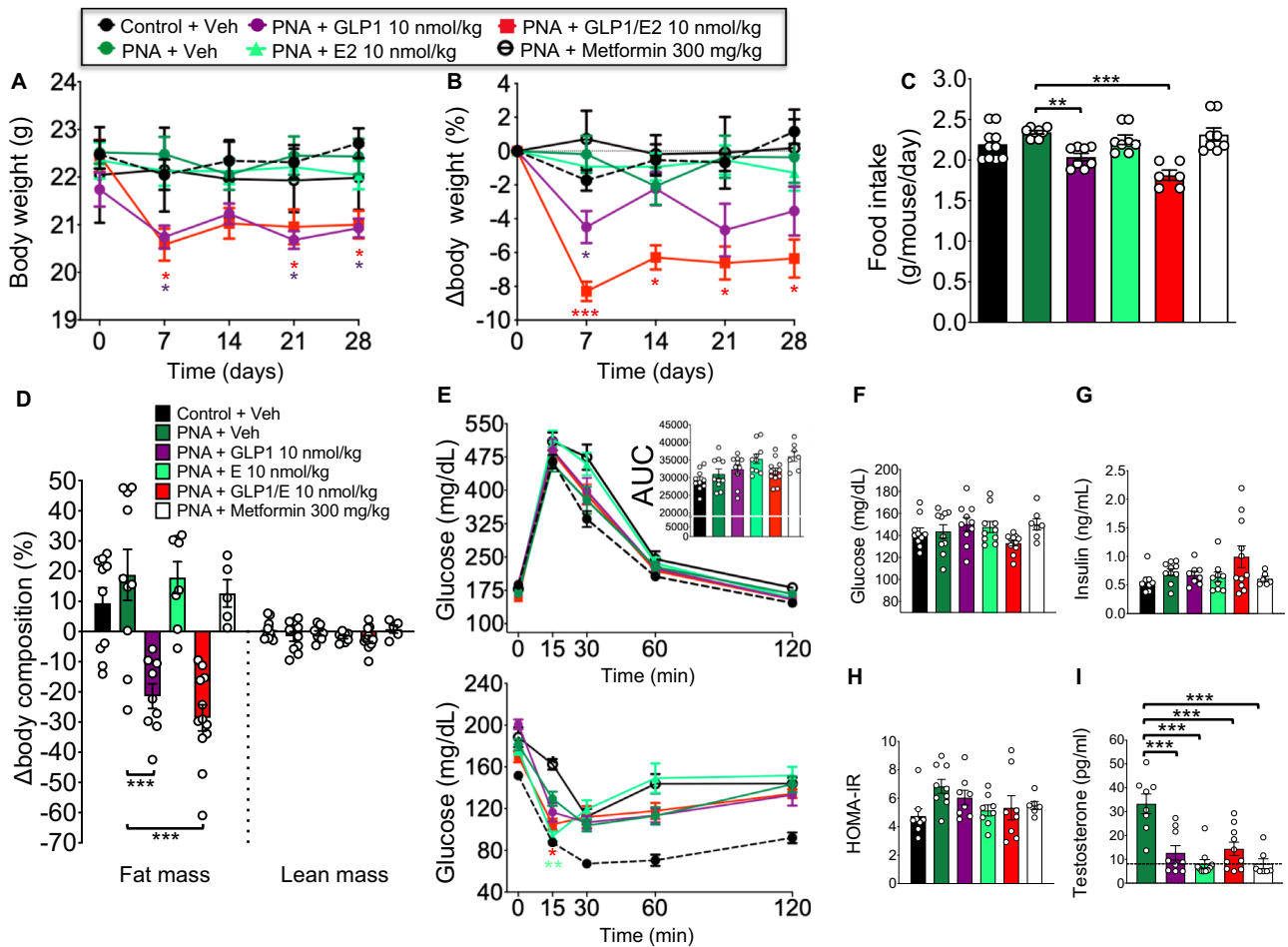


Fig. 8 | Metabolic and endocrine effects of equivalent doses of GLP1, E, or GLP1/E in PNA mice. **A–I** Effects on body weight (**A**), body weight change (**B**), food intake (**C**), body composition (fat and lean mass change) (**D**), glucose (upper panel) and insulin tolerance (**E**), fasting glucose (**F**), serum insulin levels (**G**), HOMA-IR index (**H**), and serum testosterone concentrations (**I**) in PNA female mice daily administered with vehicle (saline), GLP1 (10 nmol/kg), estrogen (E, 10 nmol/kg), GLP1/E (10 nmol/kg), or metformin (300 mg/kg) during 28 days. In order to calculate integral glucose levels in the glucose tolerance test, the area under the curve (AUC) was calculated using the trapezoidal rule. Data were presented as mean \pm SEM. Group codes: Control + Veh (C); PNA + Veh (P); PNA + GLP1 (G); PNA + E (E); PNA + GLP1/E (G/E); PNA + Metformin (M). For each panel, sample sizes (*n*) were as follows: **A:** C = 10;

P = 10; G = 10; E = 10; G/E = 11; M = 7; **B:** C = 10; P = 10; G = 10; E = 10; G/E = 11; M = 7; **C:** C = 10; P = 8; G = 8; E = 8; G/E = 6; M = 8; **D:** C = 10; P = 10; G = 9; E = 8; G/E = 12; M = 5; **E:** (GTT) C = 10; P = 10; G = 10; E = 10; G/E = 12; M = 8; (ITT) C = 10; P = 9; G = 8; E = 7; G/E = 9; M = 7; **F:** C = 10; P = 10; G = 10; E = 10; G/E = 12; M = 7; **G:** C = 8; P = 10; G = 8; E = 9; G/E = 11; M = 6; **H:** C = 8; P = 9; G = 8; E = 8; G/E = 8; M = 6; **I:** P = 8; G = 9; E = 10; G/E = 10; M = 7. Statistically significant differences were assessed by one-way ANOVA followed by Tukey's multiple comparison tests to analyze the effects of compound intervention vs. vehicle administration in PNA mice. For reference purposes, values from control non-androgenized mice are included (black bars and dashed lines). Asterisks indicate statistical significance **P* < 0.05, ***P* < 0.01, ****P* < 0.001. Source data are provided as a Source Excel Data file (see Data availability).

significantly upregulated, while ABCB9 and RIC1 were downregulated. In the PNA group, altered patterns of protein expression were also observed, with proteins such as CPOX and DPF2 being downregulated, while AMT and GSTM3 were upregulated (Fig. 10B–right panel).

Random Forest analysis was performed to identify the most important proteins contributing to a distinction between treatment and control groups. The Out-of-Bag (OOB) error rates were 0.062 for PWA conditions and 0.125 for PNA conditions, indicating robust model performance (Fig. 10C). The most important proteins, ranked by Mean Decrease Accuracy, included RABGGTA, SRSF4, and NCEH1 for the PWA group (Fig. 10D-left panel), and CPOX, CAMK2B, and BCAP31 for the PNA group (Fig. 10D-right panel). These findings are further detailed in the boxplots, where the top significant proteins identified by Random Forest analysis demonstrated distinct expression patterns between treated and control groups. In PWA animals, intervention with GLP1/E significantly downregulated hypothalamic RABGGTA and NCEH1 expression, while SRSF4 was upregulated (Fig. 10E-left panel). In turn, in PNA mice, treatment with GLP1/E caused a significant reduction in CPOX and BCAP31 expression, and increased levels of CAMK2B

(Fig. 10E-right panel). In global terms, hypothalamic pathways involved in autophagy, neurotransmitter release, cytoskeletal remodeling (RHO GTPases signaling), vesicle-mediated transport and intracellular signaling (PI3K/AKT activation) were upregulated in PWA mice treated with GLP1/E, while pathways related with vesicle transport, oxidative stress, DNA repair, metabolism and immune system were downregulated by GLP1/E treatment (Fig. 10F-left panel). In PNA mice, GLP1/E therapy caused upregulation of pathways involved in the metabolism of non-coding RNA, estrogen-dependent gene expression, autophagy, vesicle-mediated transport, and signaling by nuclear receptors, whereas proteins related to inflammation (ROS and RNS production in phagocytes), cellular response to starvation, signaling by insulin receptor, apoptosis, and immune system were downregulated.

Discussion

PCOS is a prevalent, highly heterogeneous condition affecting women of reproductive age, frequently involving metabolic comorbidities. The diversity in clinical presentations of PCOS is likely a reflection of different pathogenic mechanisms, and has implications not only for

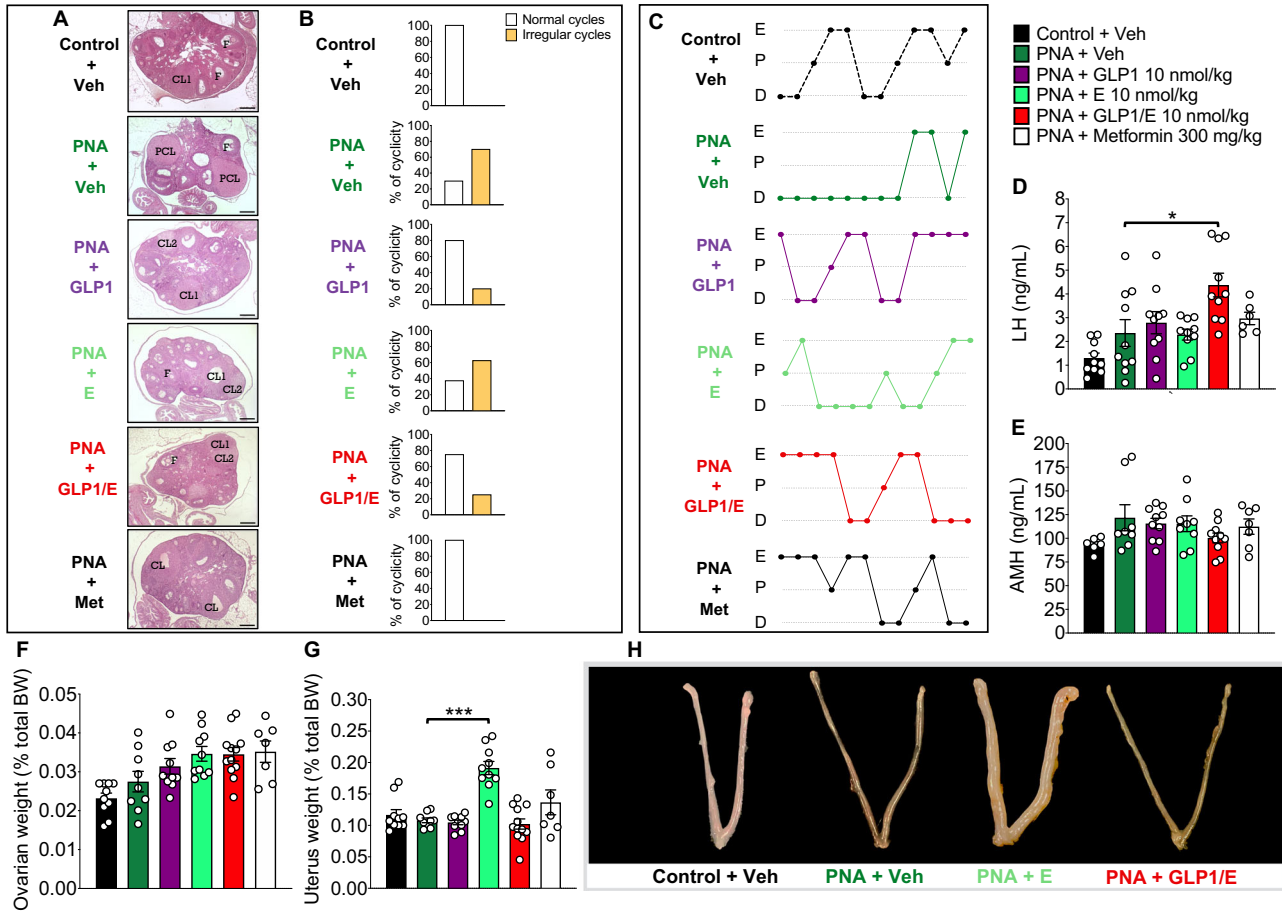


Fig. 9 | Effects of equivalent doses of GLP1, E, or GLP1/E on reproductive indices in PNA mice. **A–H** Representative images of ovarian histology (**A**), percentage of ovarian cyclicity (**B**), individual profiles of ovarian cyclicity (**C**), circulating LH levels (**D**), serum anti-Müllerian hormone (AMH) concentration (**E**), ovarian and uterus weights (**F, G**), and representative images of uterus in PNA female mice (**H**), daily treated with vehicle, GLP1 (10 nmol/kg), estrogen (10 nmol/kg), GLP1/E (10 nmol/kg), or metformin (300 mg/kg) during 28 days. Data were presented as mean ± SEM. Group codes: Control + Veh (C); PNA + Veh (P); PNA + GLP1 (G); PNA + E (E); PNA + GLP1/E (G/E); PNA + Metformin (M). For each panel, sample sizes (*n*) were as follows: **A, B:** C = 5; P' = 5; G = 5; E = 5; G/E = 5; M = 5; **C:** C = 10; P' = 9; G = 10; E = 10;

G/E = 12; M = 7; **D:** C = 10; P' = 10; G = 10; E = 10; G/E = 10; M = 6; **E:** C = 6; P' = 8; G = 10; E = 9; G/E = 10; M = 7; **F, G:** C = 10; P' = 9; G = 10; E = 10; G/E = 12; M = 7. Statistically significant differences were assessed by one-way ANOVA followed by Tukey's multiple comparison tests to analyze the effects of compound intervention vs. vehicle administration in PNA mice. For reference purposes, values from control non-androgenized mice are included (black bars and dashed lines). Asterisks indicate statistical significance **P* < 0.05, ***P* < 0.01, ****P* < 0.001. CL corpus luteum, PCL persistent corpus luteum, F follicle, E estrus, P proestrus, D diestrus. Scale bars correspond to 200 μm. Source data are provided as a Source Excel Data file (see Data availability).

timely diagnosis, but also in terms of prognosis, molecular stratification and therapeutic handling of cases. Multiple rodent models of PCOS, capitalizing mainly on the impact of androgen excess at different developmental windows, with variable penetrance in terms of reproductive and metabolic impairment, have been used in translational studies, in order to capture the phenotypic heterogeneity of the syndrome³⁸. We report herein a series of pharmacological and molecular studies in two validated mouse models of PCOS, generated by gestational (PNA) or postweaning (PWA) androgenization, addressing the effects of GLP1-based multi-agonist therapies on metabolic and reproductive traits of PCOS. Notably, the PNA model mimics a lean phenotype with subtle metabolic alterations and may phenocopy the human phenotype B of PCOS⁴⁵, characterized by hyperandrogenism and oligo-anovulation, with cycle irregularities. In contrast, PWA mice display overt metabolic perturbations, including overweight and impaired glucose homeostasis⁴⁶, and may mimic the canonical human phenotype A of PCOS linked to hyperandrogenism, anovulatory cycles, and polycystic ovarian morphology⁴⁵. To further exacerbate the metabolic compromise, the effects of the GLP1 multi-agonists were tested in androgenized animals fed on HFD. Our data delineate the therapeutic superiority of the di-agonist, GLP1/E, in the management of the

metabolic alterations of PCOS, with beneficial effects also on ovarian function in our PCOS model of preserved ovulatory function.

Currently, the available therapeutic options for the management of PCOS remain symptomatic and, in many cases, unsatisfactory. Considering that obesity and/or insulin resistance are predominant among patients with PCOS, lifestyle interventions aimed at lessening the metabolic burden of the syndrome are often at the first-line approach⁴⁵. Yet, the efficiency of such interventions is, in many cases, limited, and additional, second-line treatments are frequently implemented, that mainly involve the use of metformin, as insulin-sensitizer, with variable efficacy in terms of improvement of reproductive and metabolic alterations. Very recently, GLP1 monotherapies have also been applied in the pharmacological management of PCOS, with promising results³², which are yet to be consolidated in clinical practice. However, despite previous reports on the potential advantage posed by GLP1-based multi-agonists in the management of obesity and metabolic disease, as recently exemplified by the dramatic body weight-lowering actions of the GLP1/GIP dual agonist, tirzepatide⁴⁷, to our knowledge, no study has addressed to date the pharmacological characterization of GLP1-based unimolecular multi-agonists for management of reproductive and metabolic alterations

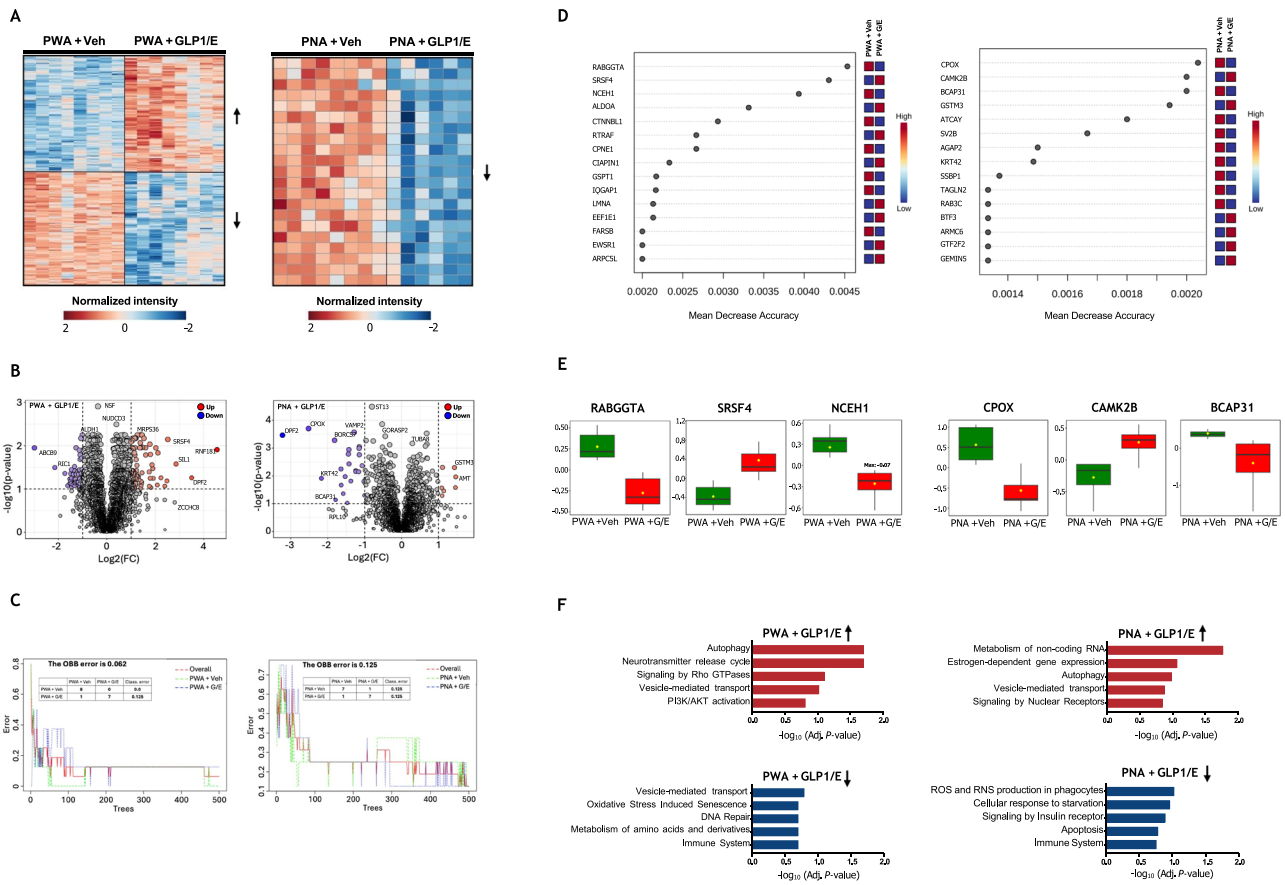


Fig. 10 | Effects of treatment with GLP1/E on hypothalamic proteome in PWA and PNA mice. A Heatmaps display the normalized intensity of protein expression across different conditions. The clustering method used is Ward, and the distance measured is Euclidean. The left heatmap compares PWA + Vehicle (control) against PWA + GLP1/E (treatment), and the right heatmap compares PNA + Vehicle (control) against PNA + GLP1/E (treatment). **B** Volcano plots illustrate the differential protein levels between treatment and control conditions. A two-sided, unpaired *t*-test was used to compare the two groups to assess significant differences in their means. The left plot shows PWA + Vehicle vs. PWA + GLP1/E, while the right plot shows PNA + Vehicle vs. PNA + GLP1/E. Proteins with significant differential expression (FDR threshold 0.1) are highlighted, with upregulated proteins in red and downregulated ones in blue. **C** Random Forest out-of-bag (OOB) error shows OOB error plots from Random Forest analysis for PWA (left) and PNA (right) conditions. The overall error, as well as errors for each specific condition (PWA+Vehicle, PWA + GLP1/E, PNA + Vehicle, and PNA + GLP1/E), are shown, indicating the model's performance and classification accuracy across different numbers of trees. **D** Variable Importance from Random Forest plots showing the mean decrease accuracy of the most important proteins identified by Random Forest analysis. The left panel represents the PWA condition, and the right panel represents the PNA. Proteins are ranked based on their importance in distinguishing between the control and treatment groups. **E** Boxplots depicting the expression levels of the most significant proteins identified by Random Forest analysis. The

three boxplots on the left show representative normalized concentrations for PWA condition (RABGGTA, SRSF4, and NCEH1), while the right set of three boxplots shows similar results for PNA (CPOX, CAMK2B, and BCAP31). For each protein, normalized expression levels are compared between Vehicle (green) and GLP1/E treatment (red) groups. The X-axis denotes the experimental groups (i.e., vehicle or GLP1/E), while the Y-axis corresponds to the normalized protein concentrations. The boxes represent the interquartile range (IQR) of the normalized values, spanning from the 25th percentile (Q1) to the 75th percentile (Q3), with the median indicated by horizontal lines. The yellow diamond denotes the mean value. The whiskers extend to the minimum and maximum values within the data distribution. **F** Selected enriched pathways upregulated and downregulated in PWA and PNA mice after intervention with GLP1/E are represented in bar graphs. The statistical test used was the hypergeometric test, adjusted using FDR. The x-axis displays the $-\log_{10}$ of the adjusted P-value. Group codes: PWA + Veh (P); PWA + GLP1/E (P + G/E); PNA + Veh (P'); PNA + GLP1/E (P' + G/E). Sample sizes (n) were as follows: **A:** (Left panel) P = 8; P + G/E = 8; (Right panel) P' = 8; P' + G/E = 8; **B:** (Left panel) P = 8; P + G/E = 8; (Right panel) P' = 8; P' + G/E = 8; **C:** (Left panel) P = 8; P + G/E = 8; (Right panel) P' = 8; P' + G/E = 8; **D:** (Left panel) P = 8; P + G/E = 8; (Right panel) P' = 8; P' + G/E = 8; **E:** (Left panel) P = 8; P + G/E = 8, (Right panel) P' = 8; P' + G/E = 8; **F:** (Left panel) P = 8; P + G/E = 8; (Right panel) P' = 8; P' + G/E = 8. MS proteomics data have been deposited to the ProteomeXchange Consortium via the PRIDE partner repository (see Data availability).

of PCOS, using suitable preclinical models, as pre-requisite for their application in clinics. Of note, most of the pharmacological testing of these GLP1-based compounds has been implemented so far in male models of obesity^{33–35,48}, with limited insight into their effects in female-specific metabolic conditions. Given the impact of androgen excess on multiple reproductive and metabolic parameters of females, such analyses are deemed mandatory in order to define the potential utility of such compounds for the personalized treatment of women suffering from PCOS.

The dose-findings studies reported here not only documented the superior efficacy of GLP1/E in the management of metabolic alterations

in our obese PCOS model, including lowering body weight and adiposity, as well as improvement of glucose handling and insulin resistance, but also highlighted a non-monotonic effect of this dual agonist in PNA mice, with optimal effects being achieved with submaximal doses. Balance between on- and off-target effects of the dual GLP1/E agonist, and the concurrence of desensitization at very high doses, might contribute to this phenomenon. Notably, considerable metabolic improvement was achieved at relatively low doses of GLP1/E, thus increasing the safety margin of this compound, which did not cause uterotrophic effects per se. Also of note, in general terms, GLP1/E was superior to GLP1/GIP in our PCOS models, despite recent promising

data on body weight loss (>20%) and metabolic improvement in people with obesity treated with tirzepatide⁴⁷, and the beneficial effects of GLP1/GIP in female mice with diet-induced obesity⁴¹. Intriguingly, GLP1/GIP had limited efficacy in our PCOS model with more severe metabolic complications, i.e., PWA mice fed HFD, suggesting that in the presence of persistently elevated androgen levels, its beneficial effects might be dampened. Interestingly, clinical trials reported to date on the effects of tirzepatide did include obese men and women, but results were not segregated by gender⁴⁷, thus making it difficult to anticipate whether a sex dimorphism exist in GLP1/GIP responses. On the other hand, while the triagonist, GLP1/GIP/Glucagon, was very effective in terms of body weight lowering, in keeping with previous references⁴², treatment of PWA mice led to a massive, likely detrimental weight loss, also at the expense of lean mass, that was not bound to clear amelioration of glucose intolerance in androgenized female mice. This is in contrast with the beneficial effects reported previously for the triagonist, in terms of reversion of adiposity excess and improved metabolic profile in diet-induced obese female mice⁴², suggesting that hyperandrogenism is bound to particular metabolic features that require specific multi-agonist treatments for maximum efficacy.

Investigation of the mechanisms underlying the beneficial metabolic effects of multi-agonist therapies, conducted in PWA mice, as a genuine model for the metabolic alterations of PCOS³⁶, revealed a predominant action in terms of suppression of food intake, with negligible effects in terms of energy expenditure, thermogenic function or locomotor activity. Admittedly, these metabolic analyses were focused on the initial phase of treatments, as this period displayed the largest changes in body weight and is less likely affected by compensatory responses, which might confound the identification of primary mechanisms. In addition, changes in respiratory quotient pointed out greater fat oxidation after multi-agonist treatments, which may contribute to the beneficial effects of the compounds in the metabolic handling of PWA mice. Interestingly, a comparison of acute metabolic responses with the chronic profiles at the end of the treatment period strongly suggests that while the different GLP1-based agonists may share primary mechanisms of action, the durability and efficiency of their long-term metabolic responses differ, with clear superiority for the GLP1/E compound. In addition, our data unambiguously documented that the effects of this and other multi-functional analogs on body weight and food intake are not merely due to food aversion or malaise linked to gastrointestinal distress, regarded as one of the main side-effects of GLP1-based therapy in humans⁴⁹.

In line with our short-term metabolic analyses, previous studies in New Zealand obese and diet-induced obese male mice suggested that GLP1/E acts primarily at central levels to reverse metabolic alterations by decreasing food intake and body weight, while the potential beneficial effects on pancreatic beta-cells were possibly secondary and indirectly-mediated^{33,48}. Similar evidence has been obtained in non-diabetic male mice³⁰ and rats⁵¹. On the latter, studies conducted using site-specific brain micro-injections and single-photon emission computed tomography documented a novel regulatory role of the hypothalamic supramammillary nucleus in the regulation of food intake and reward, posing this brain area as one of the main targets of the GLP1/E conjugate, along with the lateral hypothalamus and the nucleus of the solitary tract, whose activation may be responsible for the anorectic, weight-lowering and reward reducing effects of this multi-agonist⁵¹. Our data were congruent with those findings, suggesting that GLP1/E retains its powerful body weight-lowering effects in female models of persistent androgenization and PCOS. Interestingly, the metabolic effects of GLP1/E in PWA mice were greater than those of GLP1 or E alone, documenting the potent enhancement of the actions of the individual compounds when integrated in a single, stable molecule with dual agonist activity, also in the context of PCOS. This further supports the superiority of GLP1/E vs. GLP1 monotherapy in the pharmacological handling of metabolic complications of PCOS. The logic behind this approach is that the

concomitant activation of GLP1 and estrogen receptors may drive additional favorable effects, when compared with the individual activation of these pathways, which are known to conduct, on their own, beneficial metabolic actions on energy and glucose homeostasis⁵². While the metabolic efficacy of GLP1-RA has been extensively explored, the metabolic actions of estrogen have received less attention due to the undesirable oncogenic and reproductive effects linked to estrogen therapy. Notwithstanding, previous studies have documented beneficial effects of the activation of estrogen receptors in diet-induced obese females, by reducing body weight and fat accumulation and improving leptin resistance at central level^{33,54}. In addition, estrogen signaling has been reported to potentiate the suppressive effects of GLP1-RA on food reward⁵⁵. Thus, integration of both hormones into a single molecule may not only maximize the metabolic efficacy of the individual signals, but allow also specific delivery of estrogen into GLP1 receptor-expressing cells, avoiding potential undesired effects of estrogen on reproductive tissues, as shown also in our studies.

Intriguingly, in the two PCOS models tested, metformin was only marginally effective in improving the metabolic profile, despite the high dose used and its consideration as gold standard for the treatment of insulin resistance in women suffering PCOS. In fact, only a modest improvement in insulin resistance was consistently detected in PWA mice following treatment with metformin, as reflected by a moderately reduced HOMA-IR index. These data point to some degree of refractoriness in the metabolic responses to this insulin sensitizer in our models, which could be consistently overcome by the treatment with GLP1/E, even at low-to-moderate doses. Of note, different reports have also documented the limited efficacy of similar doses of metformin in terms of improvement of metabolic profiles in experimental models of diabetes in female rats^{36,57}, as well as in PNA mice⁵⁸, suggesting that the metabolic effects of metformin may be heterogeneous and inconsistent depending on the dose and preclinical model used.

Assuming a preferential central action of GLP1/E, we conducted label-free, quantitative proteomic analyses in the hypothalamus of the two models of PCOS, after chronic treatment with the di-agonist, as a means to disclose putative pathways for the metabolic actions of the di-agonist, and the basis for the partially differential responses between the two models of PCOS, which diverge also in terms of phenotypic presentation. Molecular hypothalamic profiling revealed common and distinct proteins and pathways being affected by GLP1/E in the two PCOS models, with a consistently higher number of individual proteins being differentially expressed (DE), either up- or down-regulated, in the hypothalamus of PWA mice treated with GLP1/E vs. PNA animals. Such molecular changes help to delineate putative mechanisms of action of the di-agonist, with consistent upregulation of factors involved in autophagy, neurotransmitter release, cytoskeletal remodeling, vesicle-mediated transport, and intracellular signaling, and downregulation of pathways related, among others, with oxidative stress, DNA repair and immune system in PWA mice, which showed consistent metabolic improvement at all doses of GLP1/E. GLP1/E therapy also elicited specific changes in the hypothalamic proteomic profile in PNA mice, upregulating proteins involved in the metabolism of non-coding RNA, signaling of nuclear receptor and estrogen-dependent gene expression and downregulating pathways involved in apoptosis, signaling by insulin receptor and cellular responses to starvation. These distinct proteomic responses in PWA vs. PNA mice may provide the basis for the differential efficiency of GLP1/E in these two PCOS models. Interestingly, however, common responses to GLP1/E were observed in both PCOS models, with upregulation of hypothalamic pathways involved in autophagy and vesicle-mediated transport, and downregulation of pathways primarily related to the immune system.

The ultimate pathways whereby these molecular changes may translate into changes in body weight and metabolic (dys)function are yet to be fully disclosed, but alterations in the hypothalamic proteome involved in inflammatory and apoptotic processes, as well as in

autophagy and vesicular trafficking, may play a role. Our proteomic data suggest that GLP1/E promotes the downregulation of proteins involved in immune response in both PCOS models. It is well known that HFD-induced obesity promotes low-grade hypothalamic inflammation, causing deregulation of central mechanisms that control energy homeostasis⁵⁹, and both physical exercise and some pharmacotherapies have been shown to improve systemic metabolism by attenuating hypothalamic inflammation^{60,61}. In addition, HFD also promotes apoptotic processes at the hypothalamic level⁶², and weight-lowering therapies, as exercise, contribute to mitigate apoptosis in hypothalamic neurons⁶⁰. In our PCOS models, GLP1/E may ameliorate hypothalamic inflammation, as reflected by a reduced expression of proteins related to the immune system, and attenuate apoptotic responses. On the latter, specific proteins involved in the activation of apoptosis, such as BCAP31, were downregulated at the hypothalamus after GLP1/E treatment. Defective hypothalamic autophagy and vesicular trafficking are also considered relevant pathogenic factors in the development of obesity^{63,64}. Activation of autophagy is regarded as a promising strategy for the prevention and treatment of metabolic diseases⁶⁵. GLP1/E therapy led to upregulation of pathways involved in autophagy and vesicle-mediated transport, suggesting that this intervention enhances hypothalamic autophagy, a mechanism that may contribute to the metabolic improvement observed in GLP1/E-treated animals. Our data also document changes in other specific hypothalamic signaling pathways that may be related to the metabolic effects of the multi-agonist, as is the case of calcium/calmodulin-dependent protein kinase 2 (CAMK2). This enzyme participates in the regulation of energy balance by modulating hypothalamic production of the orexigenic peptide NPY⁶⁶. Pharmacological inhibition of hypothalamic CAMK2 has been shown to reduce food intake and body weight by decreasing NPY expression⁶⁶. Intriguingly, in our studies, hypothalamic CAMK2 expression was upregulated by GLP1/E; an effect that may be due to compensatory mechanisms in response to the marked reduction of body weight after chronic treatment with GLP1/E. All in all, while identification of the molecular mechanisms for its beneficial metabolic effects warrants further investigation, our proteomic data strongly suggest a distinctive role of central actions of GLP1/E for the amelioration of the metabolic profiles of our PCOS models.

In parallel to their metabolic impact, the reproductive effects of the GLP1-based multi-agonists were also assessed in PNA and PWA models of PCOS, particularly for GLP1/E. Of note, the reproductive phenotype of these two models is partially divergent, mimicking conditions of cycle irregularities but preserved ovulation (PNA) or complete anovulation (PWA), which also exist in clinics among women suffering from the syndrome³⁸. For the PWA model of persistent hyperandrogenism, none of the multi-agonist was able to substantially ameliorate the state of reproductive dysfunction, as manifested by a lack of effects on sex organ weights or reproductive hormone levels, as well as by the failure to rescue ovulation. This is somewhat unsurprising, given the fact that persistently elevated androgen levels in PWA rodents have been shown to prevent ovulatory rescue after administration of more proximal activators of the reproductive axis, such as kisspeptin⁴⁶. The inability of the multi-agonists to restore gonadal function in PWA mice is likely due to chronic exposure to fixed concentrations of the exogenous androgen, DHT, which may limit the eventual beneficial effects of the compounds at the gonadal level, even when substantial metabolic improvements are achieved. Importantly, the vast majority of the available PCOS models are generated by exogenous administration of androgens during specific developmental windows, which hampers evaluation of the effects of treatments on endogenous androgen secretion and ovarian function. In addition, despite previous reports on the capacity of GLP1 on its own to activate the female reproductive axis⁶⁷, this effect was not detected in our study, with no long-term impact on LH or AMH levels, which might suggest a state of refractoriness due to persistent androgenization. However, it must be stressed that, despite the lack of reproductive

improvement, even low doses of GLP1/E were sufficient to markedly improve the metabolic perturbations in PWA mice, thus defining an optimal scenario for occasions in which the main therapeutic objective would be metabolic normalization rather than reproductive rescue, as is actually the case for most women with PCOS, without pregnancy desire, which are submitted to continued hormonal contraception plus metformin treatment. Whether this should be regarded as specific metabolic treatment, targeting only the metabolic alterations of the syndrome, is debatable, since the improvement in metabolic conditions, e.g., insulin resistance, would tenably have a positive impact also in gonadal function in women with PCOS. Anyhow, according to our preclinical data, GLP1/E may be superior in terms of metabolic handling in women with PCOS and obesity not actively seeking pregnancy, as reflected by our results in the metabolically-compromised PWA mice³⁶.

Interestingly, reproductive responses were partially different in the PCOS model of preserved ovulation, since treatment of PNA mice with a low dose of GLP1/E was capable to elevate LH levels and reversed, to a large extent, the ovarian cycle irregularities observed in PNA mice treated with vehicle. Notably, these effects were not mimicked by E alone, which failed to rescue cycle perturbations and had a discernible uterotrophic action, but were replicated, in terms of reversal of irregularities of the ovarian cycle, by GLP1 alone, which nonetheless did not elevate LH levels. Interestingly, despite the lack of consistent actions of metformin in terms of metabolic profiles, treatment with the insulin sensitizer caused a complete normalization of ovarian cyclicity, pointing to a discernible reproductive effect of metformin in some PCOS conditions, in line with clinical literature⁶⁸, although conflictive results have been reported also⁶⁹. In any event, taken as a whole, our preclinical data point out that GLP1/E-based therapies would be superior than metformin also for an integral management of the metabolic and reproductive complications of milder cases of PCOS, with less severe metabolic alterations and preserved ovulatory function.

In sum, our data document the beneficial effects of GLP1-based multi-agonists, and particularly GLP1/E, in two models of PCOS, with the identification of optimal doses, main metabolic and reproductive effects, and tenable hypothalamic pathways targeted. Comparison with previously reported responses to different GLP1 multi-agonists in other (non-androgenic) models of obesity (see Suppl. Table S2) clearly illustrates that the beneficial effects of GLP1/E are not merely an extension of the positive impact of GLP1-based therapies on as yet another models of obesity, but rather represent a genuine phenomenon, which sets the grounds for the therapeutic use of this novel family of unimolecular compounds with hormonal multi-agonist activity in the personalized management of PCOS.

Methods

Study approval

All the related experiments and protocols used in these studies were approved by the Ethical Committees of the University of Cordoba and Junta de Andalucía (Spain), according to EU normative for the use and care of experimental animals (EU Directive 2010/63/UE, September 2010).

Animals and diets

C57BL6/J female mice bred at the vivarium of the University of Cordoba were used. Mice were housed under stable conditions of temperature (22 ± 2 °C), humidity (20%), and light (12 h light/dark cycle), with free access to tap water and diet. As described in the results section, the animals included in the experimental design, including the non-androgenized controls, were fed a high-fat diet with 58% kcal from fat, 25.5% from carbohydrates, and 16.4% from proteins (Research Diets, D12331). This protocol was applied to exacerbate metabolic impairment in the models of PCOS, commonly seen in this syndrome, and as a means to define adverse conditions where to test the therapeutic potential of the selected multi-agonists. Yet, in

specific experiments, non-androgenized control animals, included for reference purposes, were fed a standard chow diet, with a dry matter composition of 3.5% fat, 5.9% fiber, 14% proteins, and 57.5% water-soluble carbohydrates, estimated as N-free-extracts (LASQdiet®, Rod14-R).

Experimental design

In order to generate the murine models of PCOS, C57BL/6J male and female mice were purchased from Charles River Laboratories (France). Once arrived at the vivarium of the University of Cordoba at IMIBIC, animals were housed under stable conditions. After an acclimatization period, animals were mated, and specific protocols of androgenization were applied (see below). Due to the heterogeneity in the clinical presentation of PCOS, two well-validated murine models of PCOS^{37,46,70} were used.

In detail, a PCOS model was generated by applying a prenatal androgenization (PNA) protocol. In order to generate this model and induce PCOS-like traits in adult offspring, pregnant dams were administered with a daily dose of the androgen dihydrotestosterone (DHT, 250 µg/day) during gestational days 16, 17, and 18. This androgenization protocol is sufficient to induce a PCOS-like phenotype in the female offspring, characterized by modest metabolic alterations and ovarian irregularities. Note that these animals are not permanently exposed to exogenous androgens in adulthood. In addition, a postweaning androgenization (PWA) model was generated by implantation of subcutaneous capsules containing DHT (10 mg) to female mice after weaning (day 21), thereby allowing chronic androgen exposure up to adulthood. This PWA model mimics a subtype of PCOS patients that exhibit chronic hyperandrogenism, with marked metabolic, hormonal, and reproductive/gonadal alterations, which represent the majority of cases.

In both PCOS models, dietary intervention (HFD) was initiated after weaning, whereas pharmacological treatments started on postnatal day (PND) 80. Prior to initiation of treatments, mice were randomized and distributed into groups allowing similar mean values of body weight and fat mass. Animals were daily administered (s.c.) with optimal doses of the different GLP1-based multi-agonists or vehicle (saline) for 28 consecutive days. In order to validate the PCOS models, non-androgenized controls treated with vehicle were also included in the different studies. In addition, in order to compare the pharmacological efficacy of the multi-agonists with the standard treatment, subgroups of animals were orally treated with a daily dose of metformin (300 mg/kg); a dose adjusted to that employed in humans by means of the application of the body surface area normalization method⁷¹, frequently used in rodent models^{72,73}. After chronic treatment (completed by PND108), animals were euthanized, and blood and tissue samples were collected, processed, and properly stored until analyzed. A schematic representation of the generation of the murine models of PCOS and the experimental design is depicted in Suppl. Fig. S1.

Compound synthesis and formulation

The different GLP1-based multi-agonists employed in the study, including GLP1/E, GLP1/GIP dual agonist, and GLP1/GIP/glucagon triagonist, as well as the GLP1 mono-agonist, were synthesized, purified and characterized as extensively reported elsewhere^{33–35,74}. Estrogen (17β-estradiol, Sigma-Aldrich; MO, USA) was dissolved in 100% ethanol and diluted in saline solution to the required concentration. Metformin (L,1-Dimethylbiguanide hydrochloride, Sigma-Aldrich; MO, USA) was dissolved to the necessary concentration in saline solution.

Analysis of body composition

For the determination of changes in body composition, whole-body composition (fat and lean mass) was measured prior to initiation and at the end of treatments by using nuclear magnetic resonance technology (EchoMRI; TX, USA).

Glucose and insulin tolerance tests

In order to assess the effects of the different pharmacotherapies on glucose tolerance, animals were subjected to an intraperitoneal glucose tolerance test (GTT) during the third week of treatment, 24 h after the last drug administration. Mice were fasted for 5 h at the beginning of the light cycle, and then intraperitoneally injected with 2 g of glucose per kg body weight. Glucose levels were determined in blood samples before (0) and at 15, 30, 60, and 120 min following glucose administration. For the evaluation of the effects of treatments on insulin sensitivity, insulin tolerance tests (ITT) were conducted 5 days after implementation of the GTTs, which allowed the proper recovery and washout of the animals. In this case, 5-h-fasted mice were intraperitoneally administered with 0.75 U of insulin (Sigma-Aldrich, MO, USA) per kg body weight, and blood glucose concentrations were determined before (0) and at 15, 30, 60, and 120 min after insulin injection. In both tests, circulating glucose levels were measured by using a handheld digital glucometer (Roche Diagnostics; Barcelona, Spain) in blood samples taken from the tail vein.

Calculation of HOMA-IR index

The homeostatic model assessment of insulin resistance (HOMA-IR) was calculated using the formula: $\text{HOMA-IR} = [\text{fasting insulin (mU/L)} \times \text{fasting glucose (mg/dL)}] / 405$ ⁷⁵. For calculation, 5-h fasting blood samples were collected from the tail, and glucose and insulin levels were determined using a digital glucometer (Roche) and a commercial ultrasensitive insulin ELISA kit (ALPCO; NH, USA), respectively.

Determination of circulating hormones

After euthanasia, trunk blood was collected, centrifuged at 2800×g and 4 °C for 10 min, and serum was collected and stored at –20 °C until measurements. Circulating LH levels were quantified using an ultrasensitive sandwich ELISA, following specific protocols described elsewhere⁷⁶. For the determination of serum insulin levels, a commercial ultrasensitive ELISA kit was used (ALPCO). Serum leptin and adiponectin concentrations were also measured by commercially sensitive ELISA kits (Crystal Chem; IL, USA). Similarly, AMH and FGF21 serum levels were quantified by using commercial ELISA kits provided by Ansh Labs (TX, USA) and EMD Millipore Corporation (MO, USA), respectively. All the commercial assays were performed following the protocols supplied by the manufacturer.

Evaluation of gastrointestinal distress by the multi-agonists:

Pica test

To investigate whether multi-agonist therapy is bound to gastrointestinal distress, pica tests were conducted in PWA mice treated with the multi-functional drugs. Pica test serves as an indirect indicator of nausea/malaise in non-vomiting species (e.g., mice), assessed through the ingestion of kaolin clay, a non-nutritive substance that mice instinctively consume as a response to gastrointestinal discomfort⁷⁷. PWA and control non-androgenized mice were exposed to kaolin pellets (Research Diets, K50001) 10 days prior to the start of the treatments to allow for adaptation to kaolin clay. When treatments were initiated, mice had ad libitum access to food, water, and kaolin pellets. Animals were daily administered with equivalent doses (10 nmol/kg) of GLP1/E, GLP1/GIP, or GLP1/GIP/Glucagon for 3 days. For comparative purposes, a group treated with a similar dose of a GLP1 analog and a non-androgenized control group treated with a vehicle were also included. Body weight changes were monitored daily along the treatment, and food and kaolin intakes were measured at 2-, 4-, 8-, 24-, 48-, and 72-h.

Indirect calorimetry analyses

To assess the weight-lowering mechanisms linked to multi-agonists therapy, an indirect calorimetry system Oxylet Pro™ (PANLAB; Barcelona, Spain) was used. Briefly, PWA mice were individually placed in the metabolic cages 24 h prior to initiation of the experiment to allow

for an adaptation period. After this acclimation period, mice from different groups were administered once daily with vehicle or equivalent doses (10 nmol/kg) of GLP1/E, GLP1/GIP, or GLP1/GIP/Glucagon for 3 consecutive days. During this 72-hour period, body weight and food intake were daily monitored, and oxygen consumption (VO₂) and carbon dioxide production (VCO₂) were measured every 9 min. Monitoring of VO₂ and VCO₂ allowed the calculation of energy expenditure and respiratory quotient. Home-cage locomotor activity was measured also along the treatments by means of an extensometric weight transducer integrated below each cage.

Infrared thermography

To determine the effects of multi-agonists treatment on thermogenesis, infrared pictures were taken with a handheld infrared thermal camera (FLIR Systems E54; Oregon, USA). PWA mice were placed on their cage grid, and pictures of the interscapular brown adipose tissue area were taken 6 h after acute administration with GLP1/E, GLP1/GIP, or GLP1/GIP/Glucagon (10 nmol/kg). The images were processed using the software *FLIR ResearchIR MAX* (4.40.12.38), and the mean temperature of brown adipose tissue area was represented.

Sex steroid measurements

In order to accurately perform a comprehensive analysis of sex steroid profile in both PCOS models, specific protocols of LC-MS/MS were applied as described elsewhere⁷⁸. This analytical procedure allowed accurate determination of testosterone, dihydrotestosterone, androstenedione, progesterone, 17- α hydroxyprogesterone, and estradiol levels in serum samples from PNA and PWA mice.

Ovarian histological analyses and estrous cyclicity

The dissected ovaries were fixed in a commercial Bouin solution (VWR; PA, USA) for at least 24 h. Subsequently, ovaries were processed for paraffin embedding, and sections of 10- μ m thickness were cut from each sample. The sections were stained with hematoxylin and eosin, and analyzed under the microscope. For the assessment of ovulation, the presence of corpora lutea was assessed. For evaluation of the ovarian cyclicity in the ovulatory model of PCOS, analysis of the youngest and oldest generation of corpora lutea was conducted, using validated histological protocols⁷⁹. In addition, estrous cycles were monitored by daily vaginal cytology during the last 12 days of intervention with the different compounds, using well-validated protocols for histological identification of the prototypical cellularity at each phase of the cycle.

Preparation of hypothalamic samples for LC-MS/MS analysis

For the proteomic analysis by LC-MS/MS, hypothalamic samples were dissected, immediately frozen in liquid nitrogen, and stored at -80°C until used. A total of 6–8 samples per experimental group were collected. For protein extraction, each tissue was placed into a tube containing a lysis buffer consisting of 20 mM Tris HCl with pH 7.6, 0.5 M Sucrose, 0.15 M KCl, 20 mM DTT supplemented with 100 μ L/mL of a protease inhibitor cocktail (Sigma-Aldrich, MO, USA) in a 1:3 (v/v) ratio. Then, tissues were homogenized using a pestle, and the homogenate was maintained on ice throughout the procedure to prevent protease activity. The homogenates were then centrifuged at 15,000 \times g for 20 min at 4 $^{\circ}\text{C}$ to eliminate remaining waste. Next, the supernatant was obtained by carefully removing the lipid layer and was centrifuged again at 15,000 \times g for 20 min at 4 $^{\circ}\text{C}$ to ensure all lipid phase removal. Next, all samples were precipitated and washed using a standard Methanol/Chloroform protocol adapted from previous references⁸⁰. Subsequently, total protein content was quantified by micro-fluorometry using a Qubit 2.0 Fluorometer (Invitrogen; MA, USA). Samples were then subjected to enzymatic digestion with trypsin/LysC (Preomics; Planegg, Germany) and analyzed by LC-MS/MS using an EvosepOne nanoLC (Evosep; Odense, Denmark) and a timsTOF-FLEX mass spectrometer (Bruker Daltonics; Bremen, Germany). Prior to MS

Analysis, the system was calibrated not only in mass dimension but also in ion mobility by using a spiked filter with reference calibrants (lock masses) with three Agilent ESI-L Tuning Mix ions, and the collision energy was decreased linearly from 45 eV at 1/KO = 1.30 Vs cm⁻² to 27 eV at 1/KO = 0.85 Vs cm⁻². For the DIA-PASEF method, we used the Bruker standard ‘short gradient’ method (m/z range: 475–1000 Da, 1/KO range: 0.85–1.27 Vs cm⁻², diaPASEF windows: 21 \times 25 Da).

LC-MS/MS analysis

DIA-NN 1.8 (<https://github.com/vdemichev/DiaNN/releases/tag/1.8>) was used first to build an in silico library data from the Mouse Reference Proteome (<https://www.uniprot.org/proteomes/UP000000589>, Feb 2022 version), enabling options “FASTA digest for library-free search/library generation”, “Deep learning based spectra” and “RTs and IMS prediction”. For DIA-PASEF analysis, the spectral library generated in the previous step was added. A total of 17,071 protein isoforms, 22,328 protein groups, and 347,0676 precursors in 1160,479 elution groups were used to build this library. MS1 and MS2 accuracy, and retention time window scans, were set to 0 allowing DIA-NN to perform their automatic inference using first run in the experiment (DIA-NN recommended MS1 mass accuracy setting: 12.7639 ppm). Protein inference in DIA-NN was configured to use the protein names from the FASTA file (the same FASTA file used for the spectral library generation was added) with MBR enabled. When reporting protein numbers and quantities, the Protein.Group column in DIA-NN’s report was used to identify the protein group and PG.MaxLFQ column was used to obtain the normalized quantity. The quantification mode was set to “Any LC (high accuracy)”. Following previously published recommendations, DIA-NN’s output was filtered at precursor q value <1% and global protein q value <1%. The numbers of precursors/proteins were obtained based on filtering the library for precursors within the charge range from 2 to 4 and the mass range adjusted to our acquisition scheme. All other DIA-NN settings were left default, using RT-dependent cross-run normalization and filtering the output at 1% FDR. The number of threads used by DIA-NN, were 52, and the speed and RAM option was set to Ultra-Fast.

Proteomics data analysis

A Comprehensive data management procedure encompassing three key steps was carried out to ensure the robustness and comparability of our dataset. First, for sample normalization, we employed Quantile normalization, which adjusts the data to conform to a common distribution⁸¹, thereby minimizing technical variability. Second, for data transformation, we applied a log transformation (base 10), which helps in stabilizing variance and normalizing data distribution, making the data more suitable for downstream analysis⁸². Finally, for data scaling, we used Pareto scaling, a technique where each variable is mean-centered and divided by the square root of its standard deviation. This method strikes a balance by reducing the impact of large-fold changes while preserving the inherent variability of the data.

In terms of statistical analysis, we followed two main approaches. First, we conducted a univariate analysis adjusted by false discovery rate (FDR) (p value <0.05), specifically using a Volcano plot, which combines fold change analysis and t -tests to identify significantly differentially expressed proteins. Univariate analysis provides a straightforward assessment of individual features, highlighting those with significant differences between groups. This approach is valuable for understanding specific variables that stand out on their own. Second, we employed classification and feature selection methods; in this case, we used a Random Forest algorithm that considers the inter-dependencies between features, offering insights into the combined effect of multiple variables. The Random Forest model (see <https://journal.r-project.org/articles/RN-2002-022/>) was configured with 500 trees, and the out-of-bag (OOB) error was used as a quality control metric to evaluate the model’s performance. From the Random Forest analysis, we selected the most significant proteins based on the Mean

Decrease Accuracy, which were then used for subsequent pathway analysis. Overall, the combination of these approaches (i.e., univariate analysis and Random Forest) leverages the strengths of both univariate and multivariate analyses, leading to a more robust and comprehensive understanding of the data. Finally, the pathway analysis was performed using ShinyGO v0.80⁸³ and Reactome⁸⁴ to investigate the enriched pathways associated with the significant proteins identified by the Random Forest method and Volcano plots. These analysis were carried out employing R (version 4.0.5) and subsidiary packages⁸⁵.

General statistics

Graphs and statistical analyses were performed using GraphPad Prism software V8.2.1 (Boston; MA, USA). All data are presented as the mean \pm SEM. Differences among treatment groups were considered statistically significant when $P < 0.05$ by applying a one-way ANOVA followed by Tukey's multiple comparison analysis. Markers for significance and sample sizes are shown in figure legends. Group sizes were defined based in previous analogous studies, supported also by our historical a priori power calculations and values of standard deviation obtained previously when measuring similar parameters. Animal availability for implementation of all different analytical determinations within the timeframe of our chronic experiments was also considered. As a general procedure, the investigators directly performing the experimental procedures were not blinded to the group allocation, but data analyses by senior authors were largely conducted independently to avoid potential bias.

Reporting summary

Further information on research design is available in the Nature Portfolio Reporting Summary linked to this article.

Data availability

The source data supporting the findings of this article are included in this article and its supplementary information files. The original experimental data generated in this study have been deposited in the Mendeley Data repository (<https://data.mendeley.com/datasets/7j94gwhv7/1>) under accession code <https://doi.org/10.17632/7j94gwhv7.1>. The MS proteomics data have been deposited to the ProteomeXchange Consortium via the PRIDE partner repository (<https://www.ebi.ac.uk/pride/>)⁸⁶, with the dataset identifier PXD044134. Any other information regarding the data is available from corresponding authors, upon request.

References

- Wang, R. et al. First-line ovulation induction for polycystic ovary syndrome: an individual participant data meta-analysis. *Hum. Reprod. Update* **25**, 717–732 (2019).
- Kakoly, N. S. et al. Ethnicity, obesity and the prevalence of impaired glucose tolerance and type 2 diabetes in PCOS: a systematic review and meta-regression. *Hum. Reprod. Update* **24**, 455–467 (2018).
- Ding, T. et al. The prevalence of polycystic ovary syndrome in reproductive-aged women of different ethnicity: a systematic review and meta-analysis. *Oncotarget* **8**, 96351–96358 (2017).
- Franks, S. Assessment and management of anovulatory infertility in polycystic ovary syndrome. *Endocrinol. Metab. Clin. North Am.* **32**, 639–651 (2003).
- Sanchez-Garrido, M. A. & Tena-Sempere, M. Metabolic dysfunction in polycystic ovary syndrome: pathogenic role of androgen excess and potential therapeutic strategies. *Mol. Metab.* **35**, 100937 (2020).
- Gilbert, E. W., Tay, C. T., Hiam, D. S., Teede, H. J. & Moran, L. J. Comorbidities and complications of polycystic ovary syndrome: an overview of systematic reviews. *Clin. Endocrinol.* **89**, 683–699 (2018).
- Barber, T. M. & Franks, S. Obesity and polycystic ovary syndrome. *Clin. Endocrinol.* **95**, 531–541 (2021).
- Tosi, F., Bonora, E. & Moghetti, P. Insulin resistance in a large cohort of women with polycystic ovary syndrome: a comparison between euglycaemic-hyperinsulinaemic clamp and surrogate indexes. *Hum. Reprod.* **32**, 2515–2521 (2017).
- Sirmans, S. M. & Pate, K. A. Epidemiology, diagnosis, and management of polycystic ovary syndrome. *Clin. Epidemiol.* **6**, 1–13 (2013).
- Baptiste, C. G., Battista, M. C., Trotter, A. & Baillargeon, J. P. Insulin and hyperandrogenism in women with polycystic ovary syndrome. *J. Steroid Biochem. Mol. Biol.* **122**, 42–52 (2010).
- Cadagan, D., Khan, R. & Amer, S. Thecal cell sensitivity to luteinizing hormone and insulin in polycystic ovarian syndrome. *Reprod. Biol.* **16**, 53–60 (2016).
- Jayasena, C. N. & Franks, S. The management of patients with polycystic ovary syndrome. *Nat. Rev. Endocrinol.* **10**, 624–636 (2014).
- McDonnell, T., Cussen, L., McIlroy, M. & O'Reilly, M. W. Characterizing skeletal muscle dysfunction in women with polycystic ovary syndrome. *Ther. Adv. Endocrinol. Metab.* **13**, 20420188221113140 (2022).
- Xu, Y. & Qiao, J. Association of insulin resistance and elevated androgen levels with polycystic ovarian syndrome (PCOS): a review of literature. *J. Healthc. Eng.* **2022**, 9240569 (2022).
- Kiddy, D. S. et al. Improvement in endocrine and ovarian function during dietary treatment of obese women with polycystic ovary syndrome. *Clin. Endocrinol.* **36**, 105–111 (1992).
- Huber-Buchholz, M. M., Carey, D. G. & Norman, R. J. Restoration of reproductive potential by lifestyle modification in obese polycystic ovary syndrome: role of insulin sensitivity and luteinizing hormone. *J. Clin. Endocrinol. Metab.* **84**, 1470–1474 (1999).
- Glintborg, D. & Andersen, M. Thiazolidinedione treatment in PCOS—an update. *Gynecol. Endocrinol.* **26**, 791–803 (2010).
- Nathan, N. & Sullivan, S. D. The utility of metformin therapy in reproductive-aged women with polycystic ovary syndrome (PCOS). *Curr. Pharm. Biotechnol.* **15**, 70–83 (2014).
- Mathur, R., Alexander, C. J., Yano, J., Trivax, B. & Azziz, R. Use of metformin in polycystic ovary syndrome. *Am. J. Obstet. Gynecol.* **199**, 596–609 (2008).
- Nestler, J. E. Metformin for the treatment of the polycystic ovary syndrome. *N. Engl. J. Med.* **358**, 47–54 (2008).
- Aubuchon, M. et al. Metformin does not improve the reproductive or metabolic profile in women with polycystic ovary syndrome (PCOS). *Reprod. Sci.* **16**, 938–946 (2009).
- Sturrock, N. D., Lannon, B. & Fay, T. N. Metformin does not enhance ovulation induction in clomiphene resistant polycystic ovary syndrome in clinical practice. *Br. J. Clin. Pharmacol.* **53**, 469–473 (2002).
- Legro, R. S. et al. Clomiphene, metformin, or both for infertility in the polycystic ovary syndrome. *N. Engl. J. Med.* **356**, 551–566 (2007).
- Palomba, S. et al. Prospective parallel randomized, double-blind, double-dummy controlled clinical trial comparing clomiphene citrate and metformin as the first-line treatment for ovulation induction in nonobese anovulatory women with polycystic ovary syndrome. *J. Clin. Endocrinol. Metab.* **90**, 4068–4074 (2005).
- Lashen, H. Role of metformin in the management of polycystic ovary syndrome. *Ther. Adv. Endocrinol. Metab.* **1**, 117–128 (2010).
- Muller, T. D. et al. Glucagon-like peptide 1 (GLP-1). *Mol. Metab.* **30**, 72–130 (2019).
- Fava, G. E., Dong, E. W. & Wu, H. Intra-islet glucagon-like peptide 1. *J. Diabetes Complications* **30**, 1651–1658 (2016).
- Lamos, E. M., Malek, R. & Davis, S. N. GLP-1 receptor agonists in the treatment of polycystic ovary syndrome. *Expert. Rev. Clin. Pharmacol.* **10**, 401–408 (2017).
- Rasmussen, C. B. & Lindenberg, S. The effect of liraglutide on weight loss in women with polycystic ovary syndrome: an observational study. *Front. Endocrinol.* **5**, 140 (2014).

30. Jensterle, M., Kravos, N. A., Pfeifer, M., Kocjan, T. & Janez, A. A 12-week treatment with the long-acting glucagon-like peptide 1 receptor agonist liraglutide leads to significant weight loss in a subset of obese women with newly diagnosed polycystic ovary syndrome. *Hormones* **14**, 81–90 (2015).
31. Han, Y., Li, Y. & He, B. GLP-1 receptor agonists versus metformin in PCOS: a systematic review and meta-analysis. *Reprod. Biomed. Online* **39**, 332–342 (2019).
32. Siamashvili, M. & Davis, S. N. Update on the effects of GLP-1 receptor agonists for the treatment of polycystic ovary syndrome. *Expert. Rev. Clin. Pharmacol.* **14**, 1081–1089 (2021).
33. Finan, B. et al. Targeted estrogen delivery reverses the metabolic syndrome. *Nat. Med.* **18**, 1847–1856 (2012).
34. Finan, B. et al. A rationally designed monomeric peptide triagonist corrects obesity and diabetes in rodents. *Nat. Med.* **21**, 27–36 (2015).
35. Finan, B. et al. Unimolecular dual incretins maximize metabolic benefits in rodents, monkeys, and humans. *Sci. Transl. Med.* **5**, 209ra151 (2013).
36. Osuka, S. et al. Animal models of polycystic ovary syndrome: a review of hormone-induced rodent models focused on hypothalamus-pituitary-ovary axis and neuropeptides. *Reprod. Med. Biol.* **18**, 151–160 (2019).
37. Ren, J. et al. The PNA mouse may be the best animal model of polycystic ovary syndrome. *Front. Endocrinol.* **13**, 950105 (2022).
38. Stener-Victorin, E. et al. Animal models to understand the etiology and pathophysiology of polycystic ovary syndrome. *Endocr. Rev.* <https://doi.org/10.1210/edrv/bnaa010> (2020).
39. Barrea, L. et al. PCOS and nutritional approaches: differences between lean and obese phenotype. *Metabol. Open* **12**, 100123 (2021).
40. Chudzicka-Strugala, I., Golebiewska, I., Banaszewska, B., Brudecki, G. & Zwodziazak, B. The role of individually selected diets in obese women with PCOS—a review. *Nutrients* <https://doi.org/10.3390/nu14214555> (2022).
41. Sachs, S. et al. Plasma proteome profiles treatment efficacy of incretin dual agonism in diet-induced obese female and male mice. *Diabetes Obes. Metab.* **23**, 195–207 (2021).
42. Jall, S. et al. Monomeric GLP-1/GIP/glucagon triagonism corrects obesity, hepatosteatosis, and dyslipidemia in female mice. *Mol. Metab.* **6**, 440–446 (2017).
43. Ghidewon, M. et al. Growth differentiation factor 15 (GDF15) and semaglutide inhibit food intake and body weight through largely distinct, additive mechanisms. *Diabetes Obes. Metab.* **24**, 1010–1020 (2022).
44. Borner, T. et al. GDF15 induces anorexia through nausea and emesis. *Cell Metab.* **31**, 351–362 e355 (2020).
45. Teede, H. J. et al. Recommendations from the international evidence-based guideline for the assessment and management of polycystic ovary syndrome. *Hum. Reprod.* **33**, 1602–1618 (2018).
46. Romero-Ruiz, A. et al. Kisspeptin treatment induces gonadotropic responses and rescues ovulation in a subset of preclinical models and women with polycystic ovary syndrome. *Hum. Reprod.* **34**, 2495–2512 (2019).
47. Jastreboff, A. M. et al. Tirzepatide once weekly for the treatment of obesity. *N. Engl. J. Med.* **387**, 205–216 (2022).
48. Schwenk, R. W. et al. GLP-1-oestrogen attenuates hyperphagia and protects from beta cell failure in diabetes-prone New Zealand obese (NZO) mice. *Diabetologia* **58**, 604–614 (2015).
49. Wharton, S. et al. Managing the gastrointestinal side effects of GLP-1 receptor agonists in obesity: recommendations for clinical practice. *Postgrad. Med.* **134**, 14–19 (2022).
50. Tiano, J. P., Tate, C. R., Yang, B. S., DiMarchi, R. & Mauvais-Jarvis, F. Effect of targeted estrogen delivery using glucagon-like peptide-1 on insulin secretion, insulin sensitivity and glucose homeostasis. *Sci. Rep.* **5**, 10211 (2015).
51. Vogel, H. et al. GLP-1 and estrogen conjugate acts in the supramammillary nucleus to reduce food-reward and body weight. *Neuropharmacology* **110**, 396–406 (2016).
52. Mauvais-Jarvis, F., Clegg, D. J. & Hevener, A. L. The role of estrogens in control of energy balance and glucose homeostasis. *Endocr. Rev.* **34**, 309–338 (2013).
53. Litwak, S. A. et al. Estradiol prevents fat accumulation and overcomes leptin resistance in female high-fat diet mice. *Endocrinology* **155**, 4447–4460 (2014).
54. Acharya, K. D. et al. Estradiol-mediated protection against high-fat diet induced anxiety and obesity is associated with changes in the gut microbiota in female mice. *Sci. Rep.* **13**, 4776 (2023).
55. Richard, J. E., Anderberg, R. H., Lopez-Ferreras, L., Olandersson, K. & Skibicka, K. P. Sex and estrogens alter the action of glucagon-like peptide-1 on reward. *Biol. Sex Differ.* **7**, 6 (2016).
56. Murai, Y. et al. Assessment of pharmacological responses to an anti-diabetic drug in a new obese type 2 diabetic rat model. *Med. Arch.* **71**, 380–384 (2017).
57. Toriniwa, Y. et al. Investigation of pharmacological responses to anti-diabetic drugs in female Spontaneously Diabetic Torii (SDT) fatty rats, a new nonalcoholic steatohepatitis (NASH) model. *J. Vet. Med. Sci.* **80**, 878–885 (2018).
58. Roland, A. V. & Moenter, S. M. Prenatal androgenization of female mice programs an increase in firing activity of gonadotropin-releasing hormone (GnRH) neurons that is reversed by metformin treatment in adulthood. *Endocrinology* **152**, 618–628 (2011).
59. Jais, A. & Brüning, J. C. Hypothalamic inflammation in obesity and metabolic disease. *J. Clin. Invest.* **127**, 24–32 (2017).
60. Marinho, R. et al. Endurance training prevents inflammation and apoptosis in hypothalamic neurons of obese mice. *J. Cell Physiol.* **234**, 880–890 (2018).
61. Li, X. et al. Metformin attenuates hypothalamic inflammation via downregulation of RIPK1-independent microglial necroptosis in diet-induced obese mice. *Cell Death Discov.* **7**, 338 (2021).
62. Moraes, J. C. et al. High-fat diet induces apoptosis of hypothalamic neurons. *PLoS ONE* **4**, e5045 (2009).
63. Kaushik, S. et al. Autophagy in hypothalamic AgRP neurons regulates food intake and energy balance. *Cell Metab.* **14**, 173–183 (2011).
64. Meng, Q. & Cai, D. Defective hypothalamic autophagy directs the central pathogenesis of obesity via the I κ B kinase beta (IKK-beta)/NF-kappaB pathway. *J. Biol. Chem.* **286**, 32324–32332 (2011).
65. Pietrocola, F. & Bravo-San Pedro, J. M. Targeting autophagy to counteract obesity-associated oxidative stress. *Antioxidants* <https://doi.org/10.3390/antiox10010102> (2021).
66. Anderson, K. A. et al. Hypothalamic CaMKK2 contributes to the regulation of energy balance. *Cell Metab.* **7**, 377–388 (2008).
67. Outeirino-Iglesias, V., Romani-Perez, M., Gonzalez-Matias, L. C., Vigo, E. & Mallo, F. GLP-1 increases preovulatory LH surge and the number of mature follicles, as well as synchronizing the onset of puberty in female rats. *Endocrinology* **156**, 4226–4237 (2015).
68. Notaro, A. L. G. & Neto, F. T. L. The use of metformin in women with polycystic ovary syndrome: an updated review. *J. Assist. Reprod. Genet.* **39**, 573–579 (2022).
69. Magzoub, R., Kheirleiseid, E. A. H., Perks, C. & Lewis, S. Does metformin improve reproduction outcomes for non-obese, infertile women with polycystic ovary syndrome? Meta-analysis and systematic review. *Eur. J. Obstet. Gynecol. Reprod. Biol.* **271**, 38–62 (2022).
70. Caldwell, A. S. et al. Characterization of reproductive, metabolic, and endocrine features of polycystic ovary syndrome in female hyperandrogenic mouse models. *Endocrinology* **155**, 3146–3159 (2014).
71. Reagan-Shaw, S., Nihal, M. & Ahmad, N. Dose translation from animal to human studies revisited. *FASEB J.* **22**, 659–661 (2008).

72. Di Pietro, M. et al. Metformin regulates ovarian angiogenesis and follicular development in a female polycystic ovary syndrome rat model. *Endocrinology* **156**, 1453–1463 (2015).
73. Coll, A. P. et al. GDF15 mediates the effects of metformin on body weight and energy balance. *Nature* **578**, 444–448 (2020).
74. Sachs, S. et al. Targeted pharmacological therapy restores beta-cell function for diabetes remission. *Nat. Metab.* **2**, 192–209 (2020).
75. Matthews, D. R. et al. Homeostasis model assessment: insulin resistance and beta-cell function from fasting plasma glucose and insulin concentrations in man. *Diabetologia* **28**, 412–419 (1985).
76. Steyn, F. J. et al. Development of a methodology for and assessment of pulsatile luteinizing hormone secretion in juvenile and adult male mice. *Endocrinology* **154**, 4939–4945 (2013).
77. Mitchell, D. et al. Poison induced pica in rats. *Physiol. Behav.* **17**, 691–697 (1976).
78. Ohlsson, C. et al. Low progesterone and low estradiol levels associate with abdominal aortic aneurysms in men. *J. Clin. Endocrinol. Metab.* **107**, e1413–e1425 (2022).
79. Gaytan, F. et al. Development and validation of a method for precise dating of female puberty in laboratory rodents: the puberty ovarian maturation score (Pub-Score). *Sci. Rep.* **7**, 46381 (2017).
80. Wessel, D. & Flugge, U. I. A method for the quantitative recovery of protein in dilute solution in the presence of detergents and lipids. *Anal. Biochem.* **138**, 141–143 (1984).
81. Zhao, Y., Wong, L. & Goh, W. W. B. How to do quantile normalization correctly for gene expression data analyses. *Sci. Rep.* **10**, 15534 (2020).
82. West, R. M. Best practice in statistics: the use of log transformation. *Ann. Clin. Biochem.* **59**, 162–165 (2022).
83. Ge, S. X., Jung, D. & Yao, R. ShinyGO: a graphical gene-set enrichment tool for animals and plants. *Bioinformatics* **36**, 2628–2629 (2020).
84. Fabregat, A. et al. Reactome pathway analysis: a high-performance in-memory approach. *BMC Bioinformatics* **18**, 142 (2017).
85. Xia, J., Psychogios, N., Young, N. & Wishart, D. S. MetaboAnalyst: a web server for metabolomic data analysis and interpretation. *Nucleic Acids Res.* **37**, W652–660 (2009).
86. Perez-Riverol, Y. et al. The PRIDE database resources in 2022: a hub for mass spectrometry-based proteomics evidences. *Nucleic Acids Res.* **50**, D543–D552 (2022).

Acknowledgements

This work was supported by grants BFU2017-83934-P, PID2020-118660GB-I00, and PID2021-126915 OA-I00 (Agencia Estatal de Investigación, Spain); co-funded with EU funds from FEDER (Program); project PIE14-00005 (Flexi-Met, Instituto de Salud Carlos III, Ministerio de Sanidad, Spain); Projects P12-FQM-01943 and P18-RT-4093 (Junta de Andalucía, Spain), Project 1254821 (University of Cordoba-FEDER); EU research contract GAP-2014-655232; and Miguel Servet research contract CP20/00080 (Instituto de Salud Carlos III; Ministerio de Sanidad, Spain). TDM was supported for this work by funding from the German Research Foundation (DFG TRR296, TRR152, SFB1123, and GRK 2816/1), the German Center for Diabetes Research (DZD e.V.) and the European Research Council ERC-CoG Trusted no.101044445. CIBER is an initiative of Instituto de Salud Carlos III (Ministerio de Sanidad, Spain).

Author contributions

M.A.S.-G. and V.S.-L. share the first author position based on their relevant contributions in the execution of the study. B.Y., J.D.D., B.F., and R.D.D. participated in the development and synthesis of the different multi-agonists and GLP1-RA and interpretation and discussion of results. F.R.-P., M.J.V., A.R.-M., E.T., I.V., and A.B.R. contributed to the development of the PCOS models and implementation of experiments. E.C.-G. conducted the proteomic analysis by LC-MS/MS and participated in data analysis, with in-depth proteomic data analysis and interpretation being conducted by M.M.-O. C.O. and M.P. performed the sex steroid profiling,

interpreted data, and revised the manuscript. L.P. and F.G. participated in the study design, discussion of data, and conducted histological analyses. T.D.M., R.D.D., M.H.T., and B.F. actively participated in the provision of basic reagents, the study design and interpretation of data, and critically reviewed the manuscript. M.A.S.-G. and M.T.S. should be considered as joint senior authors, with shared leading roles in terms of conceptualization of the project, study design, supervision of experiments, data interpretation and discussion, and writing of the manuscript, to whom correspondence should be addressed.

Competing interests

B.F., J.D.D., and B.Y. are former employees of Novo Nordisk. T.D.M. received funding from Novo Nordisk and speaking fees within the last 3 years from Novo Nordisk, Eli Lilly, Astra Zeneca, and Berlin Chemie AG. M.H.T. is a member of the SAB of ERX Pharmaceuticals, Inc. (last SAB meeting in 2019). Since 2018, he has served as the CSO and CEO of Helmholtz Munich (an academic research center with ca. 2500 scientists and staff). Helmholtz Munich is involved in numerous collaborations with a multitude of companies and institutions, worldwide. Cooperation, at times, involves research funding and includes (but are not limited to) interactions with e.g., Novo Nordisk, Boehringer Ingelheim, Roche Diagnostics, Arbormed, SCG Cell Therapy, and others. None of the above funding sources were involved in the preparation of this paper. M.T.S. has participated in the last 3 years in projects from Novo Nordisk and collaborated via grant agreements with the company Oxo-Life Ltd. (Barcelona, Spain), addressing therapeutic strategies for PCOS, although no connection exists between these projects/agreements and the present work. The rest of the authors have no conflict of interest to disclose in relation to the contents of this work.

Additional information

Supplementary information The online version contains supplementary material available at <https://doi.org/10.1038/s41467-024-52898-y>.

Correspondence and requests for materials should be addressed to Miguel A. Sánchez-Garrido or Manuel Tena-Sempere.

Peer review information *Nature Communications* thanks Luca Chiovato and the other, anonymous, reviewer(s) for their contribution to the peer review of this work. A peer review file is available.

Reprints and permissions information is available at <http://www.nature.com/reprints>

Publisher's note Springer Nature remains neutral with regard to jurisdictional claims in published maps and institutional affiliations.

Open Access This article is licensed under a Creative Commons Attribution-NonCommercial-NoDerivatives 4.0 International License, which permits any non-commercial use, sharing, distribution and reproduction in any medium or format, as long as you give appropriate credit to the original author(s) and the source, provide a link to the Creative Commons licence, and indicate if you modified the licensed material. You do not have permission under this licence to share adapted material derived from this article or parts of it. The images or other third party material in this article are included in the article's Creative Commons licence, unless indicated otherwise in a credit line to the material. If material is not included in the article's Creative Commons licence and your intended use is not permitted by statutory regulation or exceeds the permitted use, you will need to obtain permission directly from the copyright holder. To view a copy of this licence, visit <http://creativecommons.org/licenses/by-nc-nd/4.0/>.

© The Author(s) 2024

¹Instituto Maimónides de Investigación Biomédica de Córdoba (IMIBIC), Córdoba, Spain. ²Department of Cell Biology, Physiology and Immunology, University of Córdoba, Córdoba, Spain. ³Hospital Universitario Reina Sofía, Córdoba, Spain. ⁴CIBER Fisiopatología de la Obesidad y Nutrición, Instituto de Salud Carlos III, Córdoba, Spain. ⁵Lipids & Atherosclerosis Unit, Reina Sofia University Hospital, Córdoba, Spain. ⁶Centre for Bone and Arthritis Research, Institute of Medicine, Sahlgrenska Academy, University of Gothenburg, Gothenburg, Sweden. ⁷Research Centre for Integrative Physiology and Pharmacology, Institute of Biomedicine, University of Turku, Turku, Finland. ⁸Novo Nordisk Research Center Indianapolis, Indianapolis, IN, USA. ⁹Institute for Diabetes and Obesity, Helmholtz Zentrum München, Neuherberg, Germany. ¹⁰German Center for Diabetes Research, Neuherberg, Germany. ¹¹Walther-Straub Institute of Pharmacology and Toxicology, Ludwig-Maximilians-University, Munich, Germany. ¹²Department of Chemistry, Indiana University, Bloomington, IN, USA. ¹³Division of Metabolic Diseases, Department of Medicine, Technical University of München, Munich, Germany. ¹⁴These authors contributed equally: Miguel A. Sánchez-Garrido, Víctor Serrano-López. ¹⁵These authors jointly supervised this work: Miguel A. Sánchez-Garrido, Manuel Tena-Sempere. ✉ e-mail: b12sanom@uco.es; fi1tesem@uco.es